Drift of Spectrally Stable Shifted States on Star Graphs*

Adilbek Kairzhan†, Dmitry E. Pelinovsky†, and Roy H. Goodman‡

Abstract. When the coefficients of the cubic terms match the coefficients in the boundary conditions at a vertex of a star graph and satisfy a certain constraint, the nonlinear Schrödinger (NLS) equation on the star graph can be transformed to the NLS equation on a real line. Such balanced star graphs have appeared in the context of reflectionless transmission of solitary waves. Steady states on such balanced star graphs can be translated by an arbitrary distance along the edges and are referred to as the shifted states. When the star graph has exactly one incoming edge and several outgoing edges, the steady states are spectrally stable if their monotonic tails are located on the outgoing edges. These spectrally stable states are degenerate minimizers of the action functional with the degeneracy due to the translational symmetry. Nonlinear stability of these spectrally stable states has been an open problem up to now. In this paper, we prove that these spectrally stable states are nonlinearly unstable due to an irreversible drift along the incoming edge toward the vertex of the star graph. When the shifted states reach the vertex as a result of the drift, they become saddle points of the action functional, in which case the nonlinear instability leads to their destruction. In addition to rigorous mathematical results, we use numerical simulations to illustrate the drift instability and destruction of the shifted states on the balanced star graph.

Key words. nonlinear Schrödinger equation, orbital stability of nonlinear waves, reflectionless transmission, modulation equations, conserved quantities and symmetries

AMS subject classifications. 37K45, 35Q55

DOI. 10.1137/19M1246146

1. Introduction. *The classical Lyapunov method* establishes stability of minimizers of energy in the time flow of a dynamical system under the condition that the second variation of energy is strictly positive definite. In the context of Hamiltonian PDEs such as the nonlinear Schrödinger (NLS) equation, standing waves are often saddle points of energy but additional conserved quantities such as mass and momentum exist due to symmetries such as phase rotation and space translation. It is now a classical result [17, 37] that the standing waves are stable if they are constrained minimizers of energy when other conserved quantities are fixed and if the second variation of energy is strictly positive definite under the constraints eliminating symmetries.

Stability of standing waves in the presence of symmetries is understood in the sense of *orbital stability*, where the orbit is defined by a set of parameters along the symmetry group. Fixed values of other conserved quantities are realized by Lagrange multipliers which define

another set of parameters. Both sets of parameters (along the symmetry group and Lagrange multipliers) satisfy the modulation equations in the time flow of the Hamiltonian PDE [36]. The actual values of parameters along the symmetry group are irrelevant in the definition of an orbit for the standing waves, whereas Lagrange multipliers and the remainder terms are controlled if the second variation of energy is strictly positive under the symmetry constraints.

The present work is devoted to stability of standing waves in the NLS equation defined on a metric graph, a subject that has seen many recent developments [23]. Existence and variational characterization of standing waves was developed for star graphs [1, 2, 3, 4, 8, 9, 18] and for general metric graphs [5, 6, 7, 10, 14]. Bifurcations and stability of standing waves were further explored for tadpole graphs [24], dumbbell graphs [16, 21], double-bridge graphs [25], and periodic ring graphs [15, 26, 27]. A variational characterization of standing waves was developed for graphs with compact nonlinear core [29, 30, 34].

In the context of *star graphs*, it was realized in [5] that the infimum of energy under the fixed mass is approached by a sequence of solitary waves escaping to infinity along one edge of the star graph. Consequently, standing waves cannot be energy minimizers, as they represent saddle points of energy under the fixed mass [1]. It was shown in [19] that the second variation of energy at these standing waves is nevertheless positive but degenerates with a zero eigenvalue, hence the standing waves are saddle points beyond the second variation of energy. Orbital instability of these standing waves under the time flow of the NLS equation is developed as a result of the saddle point geometry [19].

Balanced star graphs were introduced in [33] from the condition that the NLS equation on the metric graph reduces to the NLS equation on a real line if the initial conditions satisfy certain symmetry (see also [28, 32, 38] for generalizations). Consequently, solitary waves may propagate across the vertex without any reflection. Standing waves of the NLS equation can be translated along edges of the balanced star graph with a translational parameter and are referred to as *the shifted states*. When the balanced star graph has exactly one incoming edge and several outgoing edges, according to Definition 2.1, the shifted states were proven in [20] to be spectrally stable if their monotonic tails are located on the outgoing edges (an example of such a shifted state on the balanced star graph with one incoming and three outgoing edges is shown in Figure 1). Moreover, these shifted states are constrained minimizers of the energy under fixed mass and the only degeneracies of the second variation of energy are due to phase rotation and the spatial translation of the shifted state along the balanced star graph.

Standing waves are orbitally stable in the NLS equation on a real line since the two degeneracies are related to the two symmetries of the NLS equation that correspond, via Noether's theorem, to the conservation of mass and of momentum. In contrast to this well-known result, we show in this paper that *the shifted states are orbitally unstable in the NLS equation on the balanced star graph.*

The instability is related to the following observation. The shifted state is symmetric with respect to the exchange of components on the outgoing edges. If the initial perturbation to the shifted state preserves this symmetry, then the NLS on the balanced star graph can be reduced to the NLS equation on a line, and the solution of the time evolution problem has translational symmetry. Perturbations that lack this exchange symmetry also break the translational symmetry and the solution fails to conserve momentum. Moreover, the value of the momentum functional increases monotonically in the time flow of the NLS equation and
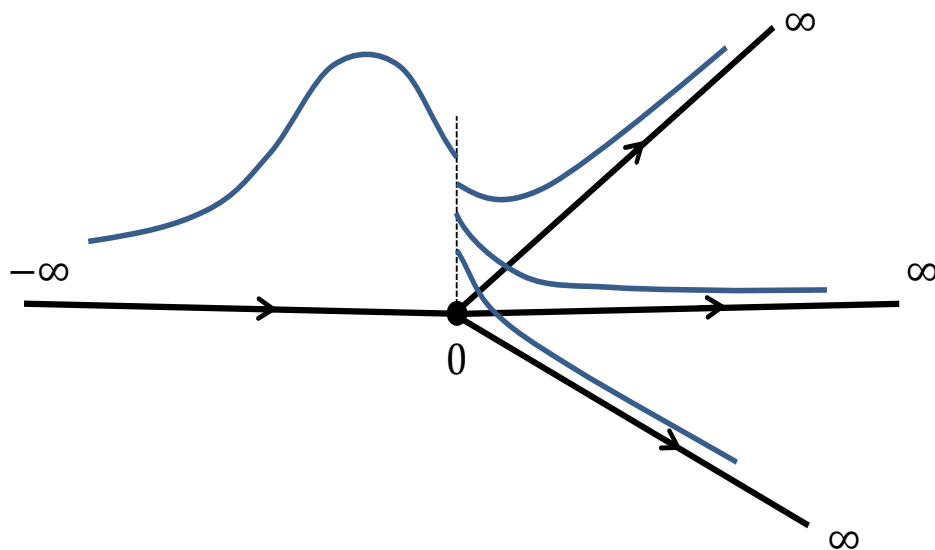
Figure 1. *A shifted state on a balanced star graph with one incoming and three outgoing edges. The shifted state has symmetric monotonic tails on the outgoing edges and a nonmonotonic tail on the incoming edge.*

this monotone increase results in the irreversible drift of the shifted state along the incoming edge toward the outgoing edges of the balanced star graph. When the center of mass of the shifted state reaches the vertex, the shifted state becomes a saddle point of energy under the fixed mass. At this point in time, orbital instability of the shifted state develops as a result of the saddle point geometry similar to the instability studied in [19].

The main novelty of this paper is to show that *degeneracy of the positive second variation of energy may lead to orbital instability of constrained minimizers if this degeneracy is not related to the symmetry of the Hamiltonian PDE*. The orbital instability appears due to irreversible drift of shifted states from a spectrally stable state toward the spectrally unstable states. We prove rigorously the conjecture posed in the previous work [20] and confirm numerically the instability of the shifted states on the balanced star graphs.

Note that the drift instability of shifted states on balanced star graphs is different from nonlinear instability of spectrally stable excited states, which are saddle points of energy subject to fixed mass [12, 13]. We emphasize again that the shifted states are degenerate minimizers of energy subject to fixed mass.

The NLS equation on a star graph is very similar to the NLS equation with a point potential supported at the vertex. This point potential repels the pinned standing wave leading to its nonlinear instability [1, 19]. Since the NLS equation on a balanced star graph can be reduced to the NLS equation on the line, one might intuitively expect stability of the standing waves as in the classical setup of [17, 37]. However, the main outcome of this work shows that topology of the balanced star graph plays the role in the time evolution of the shifted states and leads to their nonlinear instability under the symmetry-breaking perturbations.

The paper is structured as follows. Section 2 presents the background material and the main results of this work. Section 3 collects together the linear estimates. Section 4 gives the

proof of the irreversible drift along the spectrally stable shifted states. Section 5 gives the proof of nonlinear instability of the limiting point in the family of the spectrally stable shifted states (called *the half-soliton state*) due to the saddle point geometry. Section 6 illustrates the analytical results with numerical simulations. Section 7 concludes the paper with a summary.

2. Main results. We consider a *star graph* Γ constructed by attaching N half-lines at a common vertex. In the construction of the graph Γ, one edge represents an incoming bond and the remaining $N-1$ edges represent outgoing bonds. We place the vertex at the origin and parameterize the incoming edge by $\mathbb{R}^-$ and the $N-1$ outgoing edges by $\mathbb{R}^+$. The star graph Γ with one incoming and three outgoing edges is illustrated in Figure 1.

The Hilbert space

$$L^2(\Gamma) = L^2(\mathbb{R}^-) \oplus \underbrace{L^2(\mathbb{R}^+) \oplus \cdots \oplus L^2(\mathbb{R}^+)}_{\text{(N-1) elements}}$$

is defined componentwise on edges of the star graph Γ and so are Sobolev spaces

$$H^k(\Gamma) = H^k(\mathbb{R}^-) \oplus \underbrace{H^k(\mathbb{R}^+) \oplus \cdots \oplus H^k(\mathbb{R}^+)}_{\text{(N-1) elements}}$$

for $k = 1, 2$. We define function spaces H^1_Γ and H^2_Γ by using the generalized Kirchhoff boundary conditions:

$$(2.1) \qquad H^1_\Gamma := \{ \Psi \in H^1(\Gamma) : \quad \alpha_1 \psi_1(0) = \alpha_2 \psi_2(0) = \cdots = \alpha_N \psi_N(0) \}$$

and

$$(2.2) \qquad H^2_\Gamma := \left\{ \Psi \in H^2(\Gamma) \cap H^1_\Gamma : \quad \alpha_1^{-1} \psi_1'(0) = \sum_{j=2}^{N} \alpha_j^{-1} \psi_j'(0) \right\},$$

where $(\alpha_1, \alpha_2, \ldots, \alpha_N)$ are positive coefficients and derivatives are defined as $\lim_{x \to 0^-}$ for the incoming edge and $\lim_{x \to 0^+}$ for the $(N-1)$ outgoing edges. The dual space to H^1_Γ is denoted as H^{-1}_Γ.

Definition 2.1. *We say that the star graph Γ is a balanced star graph with one incoming and $N-1$ outgoing edges if the positive coefficients $(\alpha_1, \alpha_2, \ldots, \alpha_N)$ in the boundary conditions (2.1) and (2.2) satisfy the following constraint:*

$$(2.3) \qquad \frac{1}{\alpha_1^2} = \sum_{j=2}^{N} \frac{1}{\alpha_j^2}.$$

The time evolution is given by the following NLS equation:

$$(2.4) \qquad i\frac{\partial \Psi}{\partial t} = -\Delta \Psi - 2\alpha^2 |\Psi|^2 \Psi,$$

where $\Psi = \Psi(t, x)$, $\Delta \Psi = (\psi_1'', \psi_2'', \ldots, \psi_N'')$ is the Laplacian operator defined componentwise with primes denoting derivatives in x, $\alpha = (\alpha_1, \alpha_2, \ldots, \alpha_N) \in \mathbb{R}^N$ represents the same coefficients as in (2.1) and (2.2), and the nonlinear term $\alpha^2 |\Psi|^2 \Psi$ is interpreted as a symbol for

$(\alpha_1^2|\psi_1|^2\psi_1, \alpha_2^2|\psi_2|^2\psi_2, \ldots, \alpha_N^2|\psi_N|^2\psi_N)$. The Laplacian $\Delta : H_\Gamma^2 \subset L^2(\Gamma) \to L^2(\Gamma)$ is extended as a self-adjoint operator in the Hilbert space $L^2(\Gamma)$ (see Lemma 2.1 in [20]).

Local and global well-posedness of the Cauchy problem for the NLS equation (2.4) is well-known for weak solutions in H_Γ^1 (see Propositions 2.1 and 2.2 in [3] or Lemmas 2.2 and 2.3 in [20]). For the global weak solutions $\Psi \in C(\mathbb{R}, H_\Gamma^1) \cap C^1(\mathbb{R}, H_\Gamma^{-1})$, we can define the energy and mass functionals as

$$(2.5) \qquad E(\Psi) := \|\Psi'\|_{L^2(\Gamma)}^2 - \left\|\alpha^{\frac{1}{2}}\Psi\right\|_{L^4(\Gamma)}^4, \quad Q(\Psi) := \|\Psi\|_{L^2(\Gamma)}^2,$$

respectively. These functionals are constants under the time flow of the NLS equation (2.4). Similarly, one can introduce global strong solutions $\Psi \in C(\mathbb{R}, H_\Gamma^2) \cap C^1(\mathbb{R}, L^2(\Gamma))$ with conserved energy and mass functionals in (2.5).

The NLS equation (2.4) admits standing wave solutions of the form

$$\Psi(t, x) = e^{i\omega t}\Phi_\omega(x),$$

where the real-valued pair (ω, Φ_ω) satisfies the stationary NLS equation,

$$(2.6) \qquad -\Delta\Phi_\omega - 2\alpha^2|\Phi_\omega|^2\Phi_\omega = -\omega\Phi_\omega, \quad \Phi_\omega \in H_\Gamma^2.$$

The stationary NLS equation is the Euler–Lagrange equation for the action functional

$$(2.7) \qquad \Lambda_\omega(\Psi) := E(\Psi) + \omega Q(\Psi).$$

It is also well-known [3] that the set of critical points of Λ_ω in H_Γ^1 is equivalent to the set of solutions of the stationary NLS equation in H_Γ^2.

For $\omega > 0$, we can set $\omega = 1$ by employing the following scaling transformation:

$$(2.8) \qquad \Phi_\omega(x) = \omega^{\frac{1}{2}}\Phi(z), \quad z = \omega^{\frac{1}{2}}x.$$

The following lemma states the existence of a family of shifted states in the stationary NLS equation (2.6) with the boundary conditions in (2.1) and (2.2), where the coefficients $(\alpha_1, \alpha_2, \ldots, \alpha_N)$ satisfy the constraint (2.3). One such shifted state with monotonic tails on the outgoing edges of the star graph Γ is illustrated in Figure 1.

Lemma 2.2. *For every* $(\alpha_1, \alpha_2, \ldots, \alpha_N)$ *satisfying the constraint* (2.3), *there exists a unique one-parameter family of solutions* $\{\Phi(x; a)\}_{a\in\mathbb{R}}$ *to the stationary NLS equation* (2.6) *with* $\omega = 1$, *where each component of* $\Phi(x; a)$ *is given by*

$$(2.9) \qquad \phi_j(x; a) = \alpha_j^{-1}\phi(x + a), \quad 1 \le j \le n,$$

with $\phi(x) = \text{sech}(x)$.

Proof. The stationary NLS equation (2.6) with $\omega = 1$ admits a general solution $\Phi = (\phi_1, \ldots, \phi_N) \in H^2(\Gamma)$ of the form

$$\phi_j(x) = \alpha_j^{-1}\phi(x + a_j), \quad j = 1, \ldots, N,$$

with $\phi(x) = \text{sech}(x)$. The parameters $(a_1, \ldots, a_N) \in \mathbb{R}^N$ are to be defined by the boundary conditions in (2.1) and (2.2). The continuity condition in (2.1) implies that $|a_1| = \cdots = |a_N|$, and so, for every $j = 1, \ldots, N$, there exists $\sigma_j \in \{-1, 1\}$ such that $a_j = \sigma_j a_1$. Without loss of generality, we choose $\sigma_1 = 1$. The Kirchhoff condition in (2.2) implies that, under the constraint (2.3),

$$(2.10) \qquad \phi'(a_1) \sum_{j=2}^{N} \frac{\sigma_j - 1}{\alpha_j^2} = 0.$$

Equation (2.10) holds if either $\phi'(a_1) = 0$ or $\sum_{j=2}^{N} \frac{\sigma_j - 1}{\alpha_j^2} = 0$. The first case has a unique solution $a_1 = 0$. The second case holds for every $a_1 \in \mathbb{R} \backslash \{0\}$ if and only if for every $j = 2, \ldots, N$ we get $\sigma_j = 1$, since $\frac{\sigma_j - 1}{\alpha_j^2}$ is either negative or zero. Combining both cases, we have $a_1 = a_2 = \cdots = a_N = a$, where $a \in \mathbb{R}$ is arbitrary. Hence, $\Phi = (\phi_1, \phi_2, \ldots, \phi_N) \in H_\Gamma^2$ is given by (2.9). ∎

Remark 2.3. Compared to the parametrization of edges in Γ used in our previous work [20], $\phi_1(x)$ is defined here for $x \in \mathbb{R}^-$ while all other $\phi_j(x)$ are defined for $x \in \mathbb{R}^+$. We also replace parameter $a \in \mathbb{R}$ in [20] by $-a \in \mathbb{R}$ for convenience.

The shifted state (2.9) in Lemma 2.2 satisfies the following symmetry.

Definition 2.4. For every fixed $\alpha = (\alpha_1, \alpha_2, \ldots, \alpha_N)$ we say that the function $\Psi = (\psi_1, \psi_2, \ldots, \psi_N) \in H_\Gamma^1$ is α-symmetric if it satisfies for all $x \in \mathbb{R}^+$

$$(2.11) \qquad \alpha_2 \psi_2(x) = \cdots = \alpha_N \psi_N(x).$$

The symmetry (2.11) in Definition 2.4 provides the following reduction of the NLS equation (2.4) on the balanced star graph Γ under the constraint (2.3).

Lemma 2.5. *Assume that* $\Psi \in C(\mathbb{R}, H_\Gamma^2) \cap C^1(\mathbb{R}, L^2(\Gamma))$ *is a strong solution to the NLS equation* (2.4) *under the constraint* (2.3) *satisfying the symmetry reduction* (2.11) *for every* $t \in \mathbb{R}$. *The wave function*

$$(2.12) \qquad \varphi(t, x) = \begin{cases} \alpha_1 \psi_1(t, x), & x \leq 0, \\ \alpha_2 \psi_2(t, x), & x \geq 0, \end{cases}$$

is a strong solution $\varphi \in C(\mathbb{R}, H^2(\mathbb{R})) \cap C^1(\mathbb{R}, L^2(\mathbb{R}))$ *to the following NLS equation on the real line* $\mathbb{R}$:

$$(2.13) \qquad i\frac{\partial \varphi}{\partial t} = -\frac{\partial^2 \varphi}{\partial x^2} - 2|\varphi|^2 \varphi.$$

Proof. The NLS equation (2.13) is defined piecewise for $x < 0$ and $x > 0$ from the NLS equation (2.4), the symmetry (2.11), and the representation (2.12). Thanks to the boundary conditions in (2.1) and (2.2), the function $\varphi(t, x)$ is continuously differentiable across the vertex point $x = 0$. Hence if $\Psi \in C(\mathbb{R}, H_\Gamma^2) \cap C^1(\mathbb{R}, L^2(\Gamma))$ is a strong solution to (2.4), then $\varphi \in C(\mathbb{R}, H^2(\mathbb{R})) \cap C^1(\mathbb{R}, L^2(\mathbb{R}))$ is a strong solution to (2.13). ∎

Remark 2.6. The NLS equation on the line (2.13) is integrable with a Lax pair. However, the NLS equation on the star graph (2.4) is integrable only under special boundary conditions at the vertex [11] and is not integrable under the boundary conditions in (2.2) under the constraint (2.3).

The free parameter a in the family of shifted states (2.9) in Lemma 2.2 is related to the translational symmetry of the NLS equation (2.13) in x. However, the translational symmetry is broken for the NLS equation (2.4) on the star graph Γ due to the vertex at $x = 0$. As a result, the momentum functional given by

$$(2.14) \qquad P(\Psi) := \text{Im}\langle \Psi', \Psi \rangle_{L^2(\Gamma)} = \int_{\mathbb{R}^-} \text{Im}\left(\psi_1' \overline{\psi}_1\right) dx + \sum_{j=2}^{N} \int_{\mathbb{R}^+} \text{Im}\left(\psi_j' \overline{\psi}_j\right) dx$$

is no longer constant under the time flow of (2.4). It was shown in [20, Lemma 6.1] that for every strong solution $\Psi \in C(\mathbb{R}, H_\Gamma^2) \cap C^1(\mathbb{R}, L^2(\Gamma))$ to the NLS equation (2.4) the map $t \mapsto P(\Psi)$ is monotonically increasing, thanks to the following inequality:

$$(2.15) \qquad \frac{d}{dt} P(\Psi) = \frac{1}{2} \sum_{j=2}^{N} \sum_{\substack{i=2 \\ i \neq j}}^{N} \frac{\alpha_1^2}{\alpha_j^2 \alpha_i^2} \left| \alpha_j \psi_j'(0) - \alpha_i \psi_i'(0) \right|^2 \geq 0.$$

If the strong solution Ψ satisfies the symmetry (2.11) in Definition 2.4, then $P(\Psi)$ is conserved in t.

It was proven in [20, Theorem 4.1 and Corollary 4.3], that the one-parameter family of shifted states in Lemma 2.2 is spectrally unstable for $a < 0$ and spectrally stable for $a > 0$. The degenerate state at $a = 0$ is called the *half-soliton state*. For star graphs with $\alpha = 1$, the half-soliton state was proven to be nonlinearly unstable [19]. In regard to the shifted states with $a > 0$, it was conjectured in [20, Conjectures 7.1 and 7.2], that the shifted state in Lemma 2.2 with $a > 0$ is nonlinearly unstable under the time flow because the shifted states drifts along the only incoming edge toward the half-soliton state with $a = 0$, where it is affected by spectral instability of the shifted states with $a < 0$.

The present work is devoted to the proof of Conjectures 7.1 and 7.2 in [20]. We given the following definition of nonlinear instability of a shifted state $\Phi(\cdot; a)$.

Definition 2.7. *Fix* $a \in \mathbb{R}$. *The shifted state* $\Phi(\cdot; a)$ *is said to be nonlinearly unstable in* H_Γ^1 *if there exists* $\epsilon > 0$ *such that for every* $\delta > 0$ *there exists an initial datum* $\Psi_0 \in H_\Gamma^1$ *satisfying*

$$\|\Psi_0 - \Phi(\cdot; a)\|_{H^1(\Gamma)} \leq \delta$$

and $T > 0$ *such that the unique global solution* $\Psi \in C(\mathbb{R}, H_\Gamma^1) \cap C^1(\mathbb{R}, H_\Gamma^{-1})$ *to the NLS equation* (2.4) *with* $\Psi(0, \cdot) = \Psi_0$ *satisfies*

$$\inf_{\theta \in \mathbb{R}} \left\| \Psi(T, \cdot) - e^{i\theta} \Phi(\cdot; a) \right\|_{H^1(\Gamma)} > \epsilon.$$

Our first main result shows that the monotone increase of the map $t \mapsto P(\Psi)$ as in (2.15) leads to a drift along the family of shifted states (2.9) in which the parameter a decreases

monotonically in t toward $a = 0$. This drift induces nonlinear instability of the spectrally stable shifted states in Lemma 2.2 with $a > 0$ according to Definition 2.7. The following theorem formulates the result.

Theorem 2.8. *Fix $a_0 > 0$. For every $\mathfrak{a} \in (0, a_0)$ there exists $\epsilon_0 > 0$ (sufficiently small) such that for every $\epsilon \in (0, \epsilon_0)$, there exists $\delta > 0$ and $T > 0$ such that for every initial datum $\Psi_0 \in H_\Gamma^1$ satisfying*

$$(2.16) \qquad \|\Psi_0 - \Phi(\cdot; a_0)\|_{H^1(\Gamma)} \leq \delta$$

and $P(\Psi_0) \geq C_0\delta$ for some $C_0 > 0$, the unique global solution $\Psi \in C(\mathbb{R}, H_\Gamma^1) \cap C^1(\mathbb{R}, H_\Gamma^{-1})$ to the NLS equation (2.4) with $\Psi(0, \cdot) = \Psi_0$ satisfies

$$(2.17) \qquad \inf_{\theta \in \mathbb{R}} \|\Psi(t, \cdot) - e^{i\theta}\Phi(\cdot; a(t))\|_{H^1(\Gamma)} \leq \epsilon, \quad t \in [0, T],$$

where $a \in C^1([0, T])$ is a strictly decreasing function such that $\lim_{t \to T} a(t) = \mathfrak{a}$.

By Theorem 2.8, the shifted state (2.9) with $a > 0$ drifts toward the half-soliton state with $a = 0$. The half-soliton state is more degenerate than the shifted state with $a > 0$ because the zero eigenvalue of the linearized operator to the stationary NLS equation (2.6) is simple for $a > 0$ and has multiplicity $N - 1$ for $a = 0$. Moreover, while the shifted state $\Phi(\cdot; a)$ with $a > 0$ is a degenerate minimizer of the action functional $\Lambda_{\omega=1}(\Psi) = E(\Psi) + Q(\Psi)$, the half-soliton state $\Phi_0 := \Phi(\cdot; a = 0)$ is a degenerate saddle point of the same action functional [19]. The following theorem shows the nonlinear instability of the half-soliton state according to Definition 2.7. This nonlinear instability is related to the saddle point geometry of the critical point Φ_0.

Theorem 2.9. *Denote $\Phi_0 := \Phi(\cdot; a = 0)$. There exists $\epsilon > 0$ such that for every small $\delta > 0$ there exists $V \in H_\Gamma^1$ with $\|V\|_{H_\Gamma^1} \leq \delta$ such that the unique global solution $\Psi \in C(\mathbb{R}, H_\Gamma^1) \cap C^1(\mathbb{R}, H_\Gamma^{-1})$ to the NLS equation (2.4) with the initial datum $\Psi(0, \cdot) = \Phi + V$ satisfies*

$$(2.18) \qquad \inf_{\theta \in \mathbb{R}} \|e^{-i\theta}\Psi(T, \cdot) - \Phi\|_{H^1(\Gamma)} > \epsilon \quad \text{for some} \ \ T > 0.$$

Remark 2.10. The result of Theorem 2.9 is very similar to the instability result in Theorem 2.7 in [19] which was proven for the star graph Γ with $\alpha = 1$.

Finally, the shifted state $\Phi(\cdot; a)$ with $a < 0$ is a saddle point of the action functional $\Lambda_{\omega=1}(\Psi) = E(\Psi) + Q(\Psi)$. The saddle point is known to be spectrally unstable [20]. Consequently, it is also nonlinearly unstable under the time flow of the NLS equation (2.4) according to the general theory in [31].

Our numerical results collected together in section 6 illustrate all three stages of the nonlinear instability of the shifted state with $a > 0$ on the balanced star graph Γ with $N = 3$. We show the drift instability for the shifted states with $a > 0$, the weak instability of the half-soliton state with $a = 0$, and the fast exponential instability of the shifted states with $a < 0$. We also illustrate numerically that the monotonic increase of the momentum functional in (2.15) can lead to the drift instability even if the assumption $P(\Psi_0) \geq C_0\delta > 0$ of Theorem 2.8 on the initial datum Ψ_0 is not satisfied.

3. Linear estimates. Recall that the scaling transformation (2.8) transforms the normalized shifted states Φ of Lemma 2.2 to the ω-dependent family Φ_ω of the shifted states. We note the following elementary computations:

$$(3.1) \qquad D_1(\omega) = -\langle \Phi_\omega(\cdot;a), \partial_\omega \Phi_\omega(\cdot;a) \rangle_{L^2(\Gamma)} = -\frac{1}{2}\frac{d}{d\omega}\|\Phi_\omega\|^2_{L^2(\Gamma)} = -\frac{1}{2\alpha_1^2\omega^{\frac{1}{2}}}$$

and

$$(3.2) \qquad D_2(\omega) = -\langle \Phi_\omega'(\cdot;a), (\cdot + a)\Phi_\omega(\cdot;a) \rangle_{L^2(\Gamma)} = \frac{1}{2}\|\Phi_\omega\|^2_{L^2(\Gamma)} = \frac{\omega^{\frac{1}{2}}}{\alpha_1^2}.$$

We discuss separately the linearization of the shifted state with $a \neq 0$ and the half-soliton state with $a = 0$.

3.1. Linearization at the shifted state with $a \neq 0$. For every standing wave solution $\Phi_\omega(\cdot;a)$ we define two self-adjoint linear operators $L_\pm(\omega, a) : H^2_\Gamma \subset L^2(\Gamma) \to L^2(\Gamma)$ by the differential expressions:

$$(3.3) \qquad \begin{cases} L_-(\omega, a) = -\Delta + \omega - 2\alpha^2\Phi_\omega(\cdot;a)^2, \\ L_+(\omega, a) = -\Delta + \omega - 6\alpha^2\Phi_\omega(\cdot;a)^2. \end{cases}$$

The operator $L_-(\omega, a)$ acts on the imaginary part of the perturbation to $\Phi_\omega(\cdot;a)$ and the operator $L_+(\omega, a)$ acts on the real part of the perturbation; the latter operator is also the linearization operator to the stationary NLS equation (2.6). The spectrum of the self-adjoint operators $L_\pm(\omega, a)$ was studied in [20], from which we recall some basic facts.

The continuous spectrum is strictly positive thanks to the fast exponential decay of $\Phi_\omega(x;a)$ to zero as $|x| \to \infty$ and Weyl's theorem:

$$(3.4) \qquad \sigma_c(L_\pm(\omega, a)) = [\omega, \infty),$$

where $\omega > 0$. The discrete spectrum $\sigma_p(L_\pm(\omega, a)) \subset (-\infty, \omega)$ includes finitely many negative, zero, and positive eigenvalues of finite multiplicities.

Eigenvalues of $\sigma_p(L_+(\omega, a)) \subset (-\infty, \omega)$ are known in the explicit form [20]. For $\omega = 1$, these eigenvalues are given by

- a simple negative eigenvalue $\lambda_0 = -3$;
- a zero eigenvalue $\lambda = 0$ which is simple when $a \neq 0$;
- the additional eigenvalue $\lambda = \lambda_1(a)$ of multiplicity $N - 2$ given by

$$(3.5) \qquad \lambda_1(a) = -\frac{3}{2}\tanh(a)\left[\tanh(a) - \sqrt{1 + 3\operatorname{sech}(a)}\right].$$

It is negative for $a < 0$, zero for $a = 0$ and positive for $a \in (0, a_*)$, where $a_* = \tanh^{-1}(\frac{1}{\sqrt{3}}) \approx 0.66$. The eigenvalue merges into the continuous spectrum as $a \nearrow a_*$. The spectrum of $L_+(\omega, a)$ for $\omega = 1$ is illustrated in Figure 2.

Eigenvalues of $\sigma_p(L_-(\omega, a)) \subset (-\infty, \omega)$ are nonnegative and the zero eigenvalue is simple. If $a \neq 0$, the zero eigenvalues of $L_+(\omega, a)$ and $L_-(\omega, a)$ are each simple with the eigenvectors given by
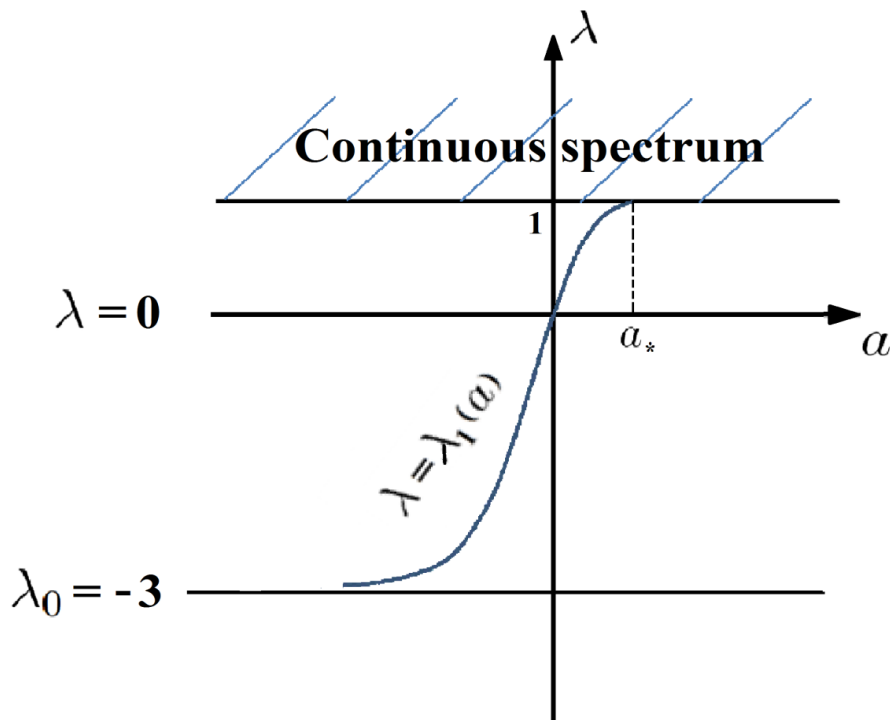
Figure 2. *The spectrum of $L_+(\omega, a)$ for $\omega = 1$. The continuous spectrum is $[1, \infty)$, while the discrete spectrum is given by the eigenvalues $\lambda = 0$, $\lambda = -3$, and $\lambda = \lambda_1(a)$ in (3.5).*

$$(3.6) \qquad L_+(\omega, a)\Phi'_\omega(\cdot; a) = 0, \quad L_-(\omega, a)\Phi_\omega(\cdot; a) = 0.$$

The eigenvectors in (3.6) induce the generalized eigenvectors in

$$(3.7) \qquad L_+(\omega, a)\partial_\omega \Phi_\omega(\cdot; a) = -\Phi_\omega(\cdot; a), \quad L_-(\omega, a)(\cdot + a)\Phi_\omega(\cdot; a) = -2\Phi'_\omega(\cdot; a).$$

The following lemma establishes the coercivity of the quadratic forms associated with the operators $L_+(\omega, a)$ and $L_-(\omega, a)$ for $a > 0$.

Lemma 3.1. *For every $\omega > 0$ and $a > 0$, there exists a positive constant $C(\omega, a)$ such that*

$$(3.8) \qquad \langle L_+(\omega, a)U, U\rangle_{L^2(\Gamma)} + \langle L_-(\omega, a)W, W\rangle_{L^2(\Gamma)} \geq C(\omega, a)\|U + iW\|^2_{H^1(\Gamma)}$$

if U and W satisfy the orthogonality conditions

$$(3.9) \qquad \begin{cases} \langle W, \partial_\omega \Phi_\omega(\cdot; a)\rangle_{L^2(\Gamma)} = 0, \\ \langle U, \Phi_\omega(\cdot; a)\rangle_{L^2(\Gamma)} = 0, \\ \langle U, (\cdot + a)\Phi_\omega(\cdot; a)\rangle_{L^2(\Gamma)} = 0, \end{cases}$$

Proof. The first orthogonality condition in (3.9) shifts the lowest (zero) eigenvalue of $L_-(\omega, a)$ to a positive eigenvalue thanks to the condition (3.1) (see Lemma 5.6 in [19]) and yields by Gårding's inequality the coercivity bound

$$\langle L_-(\omega, a)W, W\rangle_{L^2(\Gamma)} \geq C(\omega)\|W\|^2_{H^1(\Gamma)}$$

independently of a. The second orthogonality condition in (3.9) shifts the lowest (negative) eigenvalue of $L_+(\omega, a)$ to a positive eigenvalue thanks to the same condition (3.1) (see Lemma 3.8 in [19]) and yields

$$\langle L_+(\omega, a)U, U\rangle_{L^2(\Gamma)} \geq 0$$

with $\langle L_+(\omega, a)U, U\rangle_{L^2(\Gamma)} = 0$ if and only if U is proportional to $\Phi'_\omega(\cdot; a)$. The zero eigenvalue of $L_+(\omega, a)$ is preserved by the constraint since

$$\langle \Phi_\omega(\cdot; a), \Phi'_\omega(\cdot; a)\rangle_{L^2(\Gamma)} = 0.$$

Finally, the third orthogonality condition in (3.9) shifts the zero eigenvalue of $L_+(\omega, a)$ to a positive eigenvalue thanks to the condition (3.2). By Gårding's inequality, this yields the coercivity bound

$$\langle L_+(\omega, a)U, U\rangle_{L^2(\Gamma)} \geq C(\omega, a)\|U\|^2_{H^1(\Gamma)},$$

where $C(\omega, a)$ depends on a because the gap between the zero eigenvalue and the rest of the positive spectrum in $\sigma_p(L_+(\omega, a))$ exists for $a > 0$ but vanishes as $a \to 0$. ∎

Remark 3.2. For every $\omega > 0$, the positive constant $C(\omega, a)$ in (3.8) satisfies

$$C(\omega, a) \to 0 \quad \text{as} \quad a \searrow 0.$$

This is because the zero eigenvalue in $\sigma_p(L_+(\omega, a = 0))$ has multiplicity $(N-1)$ and the $(N-2)$ eigenvectors of $L_+(\omega, a = 0)$ satisfy the last two orthogonality conditions (3.9), as is seen from the explicit expressions (3.12) for eigenvectors.

Remark 3.3. For $a < 0$, the result of Lemma 3.1 is false because $\sigma_p(L_+(\omega, a))$ includes another negative eigenvalue, as is seen in Figure 2.

Remark 3.4. The orthogonality conditions in (3.9) are typically referred to as the symplectic orthogonality conditions, because they express the orthogonality of the residual terms U and W for the real and imaginary parts of the perturbation to $\Phi_\omega(\cdot; a)$ to the eigenvectors and generalized eigenvectors of the spectral stability problem expressed by $L_+(\omega, a)$ and $L_-(\omega, a)$ and the symplectic structure of the NLS equation. Compared to the classical approach of [36] that uses four orthogonality conditions and four parameters of modulated states, we do not use the orthogonality condition $\langle W, \Phi'_\omega(\cdot; a)\rangle_{L^2(\Gamma)} = 0$ and work with three parameters for modulations of the stationary state orbit $\{e^{i\theta}\Phi_\omega(\cdot; a)\}_{\theta \in \mathbb{R}, \omega \in \mathbb{R}^+, a \in \mathbb{R}^+}$. The reason for this is that the coercivity (3.8) is already obtained under the three orthogonality conditions (3.9) and that it is difficult to control the fourth parameter, corresponding to the velocity of the shifted state, with the energy method.

3.2. Linearization at the half-soliton state. For $a = 0$, we denote operators $L_\pm(\omega) \equiv L_\pm(\omega, a = 0)$. The kernel of the operator $L_+(\omega)$ is spanned by an orthogonal basis consisting of $N-1$ eigenvectors, which we denote by $\{U_\omega^{(1)}, U_\omega^{(2)}, \ldots, U_\omega^{(N-1)}\}$. The following lemma specifies an explicit construction of these basis eigenvectors.

Lemma 3.5. *There exists an orthogonal basis $\{U_\omega^{(1)}, U_\omega^{(2)}, \ldots, U_\omega^{(N-1)}\}$ of the kernel of $L_+(\omega)$ such that each eigenvector $U_\omega^{(j)}$ satisfies the orthogonality condition*

$$(3.10) \qquad\qquad\qquad\qquad\qquad \langle U, \Phi_\omega \rangle_{L^2(\Gamma)} = 0.$$

The eigenvectors can be represented as follows. For $j = 1$,

$$(3.11) \qquad\qquad\qquad U_\omega^{(1)} := \left(\alpha_1^{-1} \phi'_\omega, \alpha_2^{-1} \phi'_\omega, \dots, \alpha_N^{-1} \phi'_\omega \right),$$

and for $j = 2, \dots, N-1$,

$$(3.12) \qquad U_\omega^{(j)} := \left(\underbrace{0, \dots, 0}_{\text{(j-1) elements}}, r_j \phi'_\omega, \alpha_{j+1}^{-1} \phi'_\omega, \dots, \alpha_N^{-1} \phi'_\omega \right), \qquad r_j = - \left(\sum_{i=j+1}^N \frac{1}{\alpha_i^2} \right) \alpha_j,$$

where $\phi_\omega(x) = \omega^{\frac{1}{2}} \operatorname{sech}(\omega^{\frac{1}{2}} x)$, $x \in \mathbb{R}$.

Proof. Let $U = (u_1, u_2, \dots, u_N) \in H_\Gamma^2$ be an eigenvector for the zero eigenvalue of the operator $L_+(\omega)$. Each component of the eigenvalue problem $L_+(\omega) U = 0$ satisfies

$$(3.13) \qquad\qquad -u_j''(x) + \omega u_j(x) - 6\omega \operatorname{sech}^2 \left(\sqrt{\omega} x \right) u_j(x) = 0,$$

where $x \in \mathbb{R}^-$ on the first edge and $x \in \mathbb{R}^+$ on the remaining edges. Since $H^2(\mathbb{R}^\pm)$ are continuously embedded into $C^1(\mathbb{R}^\pm)$, if $U \in H^2(\Gamma)$, then both $u_j(x)$ and $u_j'(x)$ decay to zero as $|x| \to \infty$. Such solutions to the differential equations (3.13) are given uniquely by $u_j(x) = a_j \phi'_\omega(x)$ up to multiplication by a constant a_j. Therefore, the eigenvector U is given by

$$(3.14) \qquad\qquad\qquad U = (a_1 \phi'_\omega, a_2 \phi'_\omega, \dots, a_N \phi'_\omega).$$

The eigenvector $U \in H_\Gamma^2$ must satisfy the boundary conditions in (2.2). The continuity conditions hold since $\phi'_\omega(0) = 0$, whereas the Kirchhoff condition implies

$$(3.15) \qquad\qquad\qquad \frac{a_1}{\alpha_1} = \sum_{j=2}^N \frac{a_j}{\alpha_j}.$$

Since the scalar equation (3.15) relates N unknowns, the space of solutions for $(a_1, a_2, \dots, a_N)$ is $(N-1)$-dimensional and the kernel of the operator $L_+(\omega)$ is $(N-1)$-dimensional. Let $\{U_\omega^{(1)}, U_\omega^{(2)}, \dots, U_\omega^{(N-1)}\}$ be an orthogonal basis of the kernel, which can be constructed from any set of basis vectors by applying the Gram–Schmidt orthogonalization process.

Direct computations show that if U is given by (3.14), then

$$\langle U, \Phi_\omega \rangle_{L^2(\Gamma)} = \left(\sum_{j=2}^N \frac{a_j}{\alpha_j} - \frac{a_1}{\alpha_1} \right) \langle \phi'_\omega, \phi_\omega \rangle_{L^2(\mathbb{R}^+)},$$

which means that the condition (3.15) is equivalent to $\langle U, \Phi_\omega \rangle_{L^2(\Gamma)} = 0$. Therefore, all elements in the orthogonal basis satisfy the orthogonality condition (3.10).

It remains to prove that the orthogonal basis can be characterized in the form given in (3.11)–(3.12). From the constraint (2.3), we can take $a_j = \alpha_j^{-1}$ for all j in (3.15) to set the first eigenvector $U_\omega^{(1)}$ to be defined by (3.11). The last eigenvector $U_\omega^{(N-1)}$ can be defined by

(3.16) $$U_\omega^{(N-1)} := \left(0, \ldots, 0, r_{N-1}\phi_\omega', \alpha_N^{-1}\phi_\omega'\right),$$

where r_{N-1} is chosen to satisfy the orthogonality condition $\langle U_\omega^{(1)}, U_\omega^{(N-1)}\rangle_{L^2(\Gamma)} = 0$ and the condition (3.15). In fact, both conditions are equivalent since the first $(N-2)$ entries of $U_\omega^{(N-1)}$ are zero and

$$\left\langle U_\omega^{(1)}, U_\omega^{(N-1)}\right\rangle_{L^2(\Gamma)} = \|\phi_\omega'\|_{L^2(\mathbb{R}^+)}^2 \left(\frac{r_{N-1}}{\alpha_{N-1}} + \frac{1}{\alpha_N^2}\right)$$

with $\|\phi_\omega'\|_{L^2(\mathbb{R}^+)}^2 \neq 0$. Hence r_{N-1} is defined by

$$r_{N-1} = -\frac{\alpha_{N-1}}{\alpha_N^2}.$$

The remaining eigenvectors $U_\omega^{(j)}$ in (3.12) are constructed recursively from $j = N-2$ to $j = 2$. By direct computations we obtain that the orthogonality condition $\langle U_\omega^{(1)}, U_\omega^{(j)}\rangle_{L^2(\Gamma)} = 0$ is equivalent to the constraint (3.15). Moreover, all the eigenvectors are mutually orthogonal thanks to the recursive construction of $U_\omega^{(j)}$,   ■

We denote the kernel of $L_+(\omega)$ by

(3.17) $$X_\omega := \mathrm{span}\left\{U_\omega^{(1)}, U_\omega^{(2)}, \ldots, U_\omega^{(N-1)}\right\}.$$

For each $j = 1, 2, \ldots, N-1$, we construct the generalized eigenvector $W_\omega^{(j)} \in H_\Gamma^2$ by solving

$$L_-(\omega)W_\omega^{(j)} = U_\omega^{(j)},$$

which exists thanks to the orthogonality condition (3.10) since Φ_ω spans the kernel of $L_-(\omega)$. Explicitly, representing $U_\omega^{(j)}$ from (3.11)–(3.12) by

(3.18) $$U_\omega^{(j)} = \phi_\omega' e_j$$

with some x-independent vectors $e_j \in \mathbb{R}^N$, we get for the same vectors e_j

(3.19) $$W_\omega^{(j)} = \chi_\omega e_j,$$

where $\chi_\omega(x) = -\frac{1}{2}x\phi_\omega(x)$, $x \in \mathbb{R}$. We denote the generalized kernel of $L_-(\omega)$ by

(3.20) $$X_\omega^* := \mathrm{span}\left\{W_\omega^{(1)}, W_\omega^{(2)}, \ldots, W_\omega^{(N-1)}\right\}.$$

Similarly to Lemma 5.4 in [19], the following lemma establishes the coercivity of the quadratic forms associated with the operators $L_+(\omega)$ and $L_-(\omega)$.

Lemma 3.6. *For every $\omega > 0$, there exists a positive constant $C(\omega)$ such that*

(3.21) $$\langle L_+(\omega)U, U\rangle_{L^2(\Gamma)} + \langle L_-(\omega)W, W\rangle_{L^2(\Gamma)} \geq C(\omega)\|U + iW\|_{H^1(\Gamma)}^2$$

if $U \in X_\omega^*$ and $W \in X_\omega$ satisfy the additional orthogonality conditions

(3.22) $$\begin{cases} \langle W, \partial_\omega\Phi_\omega\rangle_{L^2(\Gamma)} = 0, \\ \langle U, \Phi_\omega\rangle_{L^2(\Gamma)} = 0. \end{cases}$$

Proof. We claim that basis vectors in X_ω and X_ω^* satisfy the following orthogonality conditions:

- $\{\langle U_\omega^{(j)}, U_\omega^{(k)} \rangle_{L^2(\Gamma)}\}_{1 \leq j,k \leq N-1}$ is a positive diagonal matrix;
- $\{\langle W_\omega^{(j)}, W_\omega^{(k)} \rangle_{L^2(\Gamma)}\}_{1 \leq j,k \leq N-1}$ is a positive diagonal matrix;
- $\{\langle U_\omega^{(j)}, W_\omega^{(k)} \rangle_{L^2(\Gamma)}\}_{1 \leq j,k \leq N-1}$ is a positive diagonal matrix.

Indeed, the orthogonality of $\{U_\omega^{(1)}, \ldots, U_\omega^{(N-1)}\}$ is established by Lemma 3.5. Therefore, the vectors $\{e_1, \ldots, e_{N-1}\}$ in (3.18) are orthogonal in $\mathbb{R}^{N-1}$. The orthogonality of $\{W_\omega^{(1)}, \ldots, W_\omega^{(N-1)}\}$ follows by the explicit representation (3.19) due to the orthogonality of the vectors $\{e_1, \ldots, e_{N-1}\}$ in $\mathbb{R}^{N-1}$. The sets $\{U_\omega^{(1)}, \ldots, U_\omega^{(N-1)}\}$ and $\{W_\omega^{(1)}, \ldots, W_\omega^{(N-1)}\}$ are mutually orthogonal by the same reason. Finally, we have for every $j = 1, \ldots, N$

$$(3.23) \qquad \left\langle U_\omega^{(j)}, W_\omega^{(j)} \right\rangle_{L^2(\Gamma)} = \frac{\alpha_j^2}{4} \left(\sum_{i=j}^{N} \frac{1}{\alpha_i^2} \right) \left(\sum_{i=j+1}^{N} \frac{1}{\alpha_i^2} \right) \|\phi_\omega\|_{L^2(\mathbb{R}^+)}^2 > 0.$$

The rest of the proof is similar to the proof of Lemma 3.1 with the only difference being that the third orthogonality condition (3.9) is replaced by the $(N-1)$ orthogonality conditions in $U \in X_\omega^*$. The constraint $U \in X_\omega^*$ provides the shift of the zero eigenvalue of $L_+(\omega)$ of algebraic multiplicity $(N-1)$ to positive eigenvalues thanks to the condition that $\{\langle U_\omega^{(j)}, W_\omega^{(k)} \rangle_{L^2(\Gamma)}\}_{1 \leq j,k \leq N-1}$ is a positive diagonal matrix. ∎

4. Drift of the shifted states with $a > 0$. The proof of Theorem 2.8 is divided into several steps. First, we decompose the unique global solution Ψ to the NLS equation (2.4) into the modulated stationary state $\{e^{i\theta}\Phi_\omega(\cdot; a)\}_{\theta \in \mathbb{R}, \omega \in \mathbb{R}^+, a \in \mathbb{R}}$ and the symplectically orthogonal remainder terms. Second, we estimate the rate of change of the modulation parameter $a(t)$ in time t and show that $a'(t) < 0$ for $t > 0$. Third, we use energy estimates to control the time evolution of the modulation parameter $\omega(t)$ and the remainder terms. Although the decomposition works for any $a(t)$, we only consider $a(t) > 0$ in order to use the coercivity bound in Lemma 3.1.

4.1. Step 1: Symplectically orthogonal decomposition. Any point in H_Γ^1 close to an orbit $\{e^{i\theta}\Phi(\cdot; a_0)\}_{\theta \in \mathbb{R}}$ for some $a_0 \in \mathbb{R}$ can be represented by a superposition of a point on the family $\{e^{i\theta}\Phi_\omega(\cdot; a)\}_{\theta \in \mathbb{R}, \omega \in \mathbb{R}^+, a \in \mathbb{R}}$ and a symplectically orthogonal remainder term. Here and in what follows, we denote $\Phi \equiv \Phi_{\omega=1}$. The following lemma provides details of this symplectically orthogonal decomposition.

Lemma 4.1. *Fix $a_0 \in \mathbb{R}$. There exists some $\delta_0 > 0$ such that for every $\Psi \in H_\Gamma^1$ satisfying*

$$(4.1) \qquad \delta := \inf_{\theta \in \mathbb{R}} \|\Psi - e^{i\theta}\Phi(\cdot; a_0)\|_{H^1(\Gamma)} \leq \delta_0,$$

there exists a unique choice for real-valued $(\theta, \omega, a) \in \mathbb{R} \times \mathbb{R}^+ \times \mathbb{R}$ and real-valued $(U, W) \in H_\Gamma^1 \times H_\Gamma^1$ in the decomposition

$$(4.2) \qquad \Psi(x) = e^{i\theta} \left[\Phi_\omega(x; a) + U(x) + iW(x) \right],$$

subject to the orthogonality conditions

(4.3)
$$\begin{cases} \langle W, \partial_\omega \Phi_\omega(\cdot; a) \rangle_{L^2(\Gamma)} = 0, \\ \langle U, \Phi_\omega(\cdot; a) \rangle_{L^2(\Gamma)} = 0, \\ \langle U, (\cdot + a)\Phi_\omega(\cdot; a) \rangle_{L^2(\Gamma)} = 0, \end{cases}$$

where ω, a, and (U, W) satisfy the estimate

(4.4)
$$|\omega - 1| + |a - a_0| + \|U + iW\|_{H^1(\Gamma)} \le C\delta$$

for some positive constant $C > 0$. Moreover, the map from $\Psi \in H^1_\Gamma$ to $(\theta, \omega, a) \in \mathbb{R} \times \mathbb{R}^+ \times \mathbb{R}$ and $(U, W) \in H^1_\Gamma \times H^1_\Gamma$ is C^ω.

   Proof. Define the following vector function $G(\theta, \omega, a; \Psi) : \mathbb{R} \times \mathbb{R}^+ \times \mathbb{R} \times H^1_\Gamma \mapsto \mathbb{R}^3$ given by

$$G(\theta, \omega, a; \Psi) := \begin{bmatrix} \langle \mathrm{Im}(\Psi - e^{i\theta}\Phi_\omega(\cdot; a)), \partial_\omega \Phi_\omega(\cdot; a) \rangle_{L^2(\Gamma)} \\ \langle \mathrm{Re}(\Psi - e^{i\theta}\Phi_\omega(\cdot; a)), \Phi_\omega(\cdot; a) \rangle_{L^2(\Gamma)} \\ \langle \mathrm{Re}(\Psi - e^{i\theta}\Phi_\omega(\cdot; a)), (\cdot + a)\Phi_\omega(\cdot; a) \rangle_{L^2(\Gamma)} \end{bmatrix},$$

the zeros of which represent the orthogonality constraints in (4.3).

   Let θ_0 be the argument of $\inf_{\theta \in \mathbb{R}} \|\Psi - e^{i\theta}\Phi(\cdot; a_0)\|_{H^1(\Gamma)}$ for a given $\Psi \in H^1_\Gamma$. The vector function $G(\theta, \omega, a; \Psi)$ is a C^ω map from $\mathbb{R} \times \mathbb{R}^+ \times \mathbb{R} \times H^1_\Gamma$ to $\mathbb{R}^3$ since the map $\mathbb{R}^+ \times \mathbb{R} \ni (\omega, a) \mapsto \Phi_\omega(\cdot; a) \in L^2(\Gamma)$ is C^ω in both variables. Moreover, if $\Psi \in H^1_\Gamma$ satisfies (4.1), then

(4.5)
$$\|G(\theta_0, 1, a_0; \Psi)\|_{\mathbb{R}^3} \le C\delta$$

for a δ-independent constant $C > 0$. Also we have

$$D_{(\theta, \omega, a)}G(\theta_0, 1, a_0; \Psi) = D + B,$$

where $D = \mathrm{diag}(d_1, d_1, d_2)$ with entries $d_1 \equiv D_1(\omega = 1)$ and $d_2 \equiv D_2(\omega = 1)$ given by (3.1) and (3.2), whereas B is a matrix satisfying the estimate $\|B\|_{\mathbb{M}_{3 \times 3}} \le C\delta$ for a δ-independent constant $C > 0$. Since $d_1, d_2 \ne 0$, the matrix D is invertible and there exists $\delta_0 > 0$ such that the Jacobian $D_{(\theta, \omega, a)}G(\theta_0, 1, a_0; \Psi)$ is invertible for every $\delta \in (0, \delta_0)$ with the bound

(4.6)
$$\|[D_{(\theta, \omega, a)}G(\theta_0, 1, a_0; \Psi)]^{-1}\|_{\mathbb{M}_{3 \times 3}} \le C$$

for a δ-independent constant $C > 0$. By the local inverse mapping theorem, for the given $\Psi \in H^1_\Gamma$ satisfying (4.1), the equation $G(\theta, \omega, a; \Psi) = 0$ has a unique solution $(\theta, \omega, a) \in \mathbb{R}^3$ in a neighborhood of the point $(\theta_0, 1, a_0)$. Since $G(\theta, \omega, a; \Psi)$ is C^ω with respect to its arguments, the solution $(\theta, \omega, a) \in \mathbb{R} \times \mathbb{R}^+ \times \mathbb{R}$ is C^ω with respect to $\Psi \in H^1_\Gamma$. The Taylor expansion of $G(\theta, \omega, a; \Psi) = 0$ around $(\theta_0, 1, a_0)$,

$$G(\theta_0, 1, a_0; \Psi) + D_{(\theta, \omega, a)}G(\theta_0, 1, a_0; \Psi)(\theta - \theta_0, \omega - 1, a - a_0)^T + \mathcal{O}(|\theta - \theta_0|^2 + |\omega - 1|^2 + |a - a_0|^2),$$

together with the bounds (4.5) and (4.6), implies the bound (4.4) for $|\omega - 1|$ and $|a - a_0|$. From the decomposition (4.2), and with use of the triangle inequality for (θ, ω, a) near $(\theta_0, 1, a_0)$, it follows that U and W are uniquely defined in H^1_Γ and satisfy the bound in (4.4). In addition, $(U, W) \in H^1_\Gamma$ are C^ω with respect to $\Psi \in H^1_\Gamma$. ∎

Let the initial datum $\Psi_0 \in H^1_\Gamma$ to the Cauchy problem associated with the NLS equation (2.4) be defined in the form

$$(4.7) \qquad \Psi_0(x) = \Phi(x; a_0) + U_0(x) + iW_0(x), \quad \|U_0 + iW_0\|_{H^1(\Gamma)} \leq \delta,$$

subject to the orthogonality conditions

$$(4.8) \qquad \begin{cases} \langle W_0, \partial_\omega \Phi_\omega|_{\omega=1}(\cdot; a_0) \rangle_{L^2(\Gamma)} = 0, \\ \langle U_0, \Phi(\cdot; a_0) \rangle_{L^2(\Gamma)} = 0, \\ \langle U_0, (\cdot + a_0) \Phi(\cdot; a_0) \rangle_{L^2(\Gamma)} = 0. \end{cases}$$

Remark 4.2. By Lemma 4.1, the orthogonal decomposition (4.7) with (4.8) implies that $\theta(0) = 0$, $\omega(0) = 1$, and $a(0) = a_0$ initially. Although this is not the most general case for the initial datum satisfying (2.16), this simplification is used to illustrate the proof of Theorem 2.8. A generalization for initial datum $\Psi_0 \in H^1_\Gamma$ with $\theta(0) \neq 0$, $\omega(0) \neq 1$, and $a(0) \neq a_0$ is straightforward.

By the well-posedness theory [3, 20], the NLS equation (2.4) with the initial datum $\Psi_0 \in H^1_\Gamma$ generates the unique global solution $\Psi \in C(\mathbb{R}, H^1_\Gamma) \cap C^1(\mathbb{R}, H^{-1}_\Gamma)$. By continuous dependence of the solution on the initial datum and by Lemma 4.1, for every $\epsilon \in (0, \delta_0)$ with δ_0 given in the bound (4.1) there exists $t_0 > 0$ such that the unique solution Ψ satisfies

$$(4.9) \qquad \inf_{\theta \in \mathbb{R}} \|e^{-i\theta} \Psi(t, \cdot) - \Phi\|_{H^1(\Gamma)} \leq \epsilon, \quad t \in [0, t_0],$$

and can be uniquely decomposed in the form

$$(4.10) \qquad \Psi(t, x) = e^{i\theta(t)} \left[\Phi_{\omega(t)}(x; a(t)) + U(t, x) + iW(t, x) \right],$$

subject to the orthogonality conditions

$$(4.11) \qquad \begin{cases} \langle W(t, \cdot), \partial_\omega \Phi_\omega|_{\omega=\omega(t)}(\cdot; a(t)) \rangle_{L^2(\Gamma)} = 0, \\ \langle U(t, \cdot), \Phi_{\omega(t)}(\cdot; a(t)) \rangle_{L^2(\Gamma)} = 0, \\ \langle U(t, \cdot), (\cdot + a(t)) \Phi_\omega(\cdot; a(t)) \rangle_{L^2(\Gamma)} = 0. \end{cases}$$

By the smoothness of the map in Lemma 4.1 and by the well-posedness of the time flow of the NLS equation (2.4), we have $U, W \in C([0, t_0], H^1_\Gamma) \cap C^1([0, t_0], H^{-1}_\Gamma)$ and $(\theta, \omega, a) \in C^1([0, t_0], \mathbb{R} \times \mathbb{R}^+ \times \mathbb{R})$.

In order to prove Theorem 2.8, we control $\omega(t)$, $U(t, \cdot)$, and $W(t, \cdot)$ from energy estimates and $a(t)$ from modulation equations, whereas $\theta(t)$ plays no role in the bound (2.17). Note that the modulation of $a(t)$ captures the irreversible drift of the shifted states along the incoming edge toward the vertex of the balanced star graph. We would not see this drift without using the parameter $a(t)$ and we would not be able to control $\omega(t)$, $U(t, \cdot)$, and $W(t, \cdot)$ from energy estimates without the third constraint in (4.11) because of the zero eigenvalue of $L_+(\omega, a)$; see Lemma 3.1.

4.2. Step 2: Monotonicity of $a(t)$. We use the orthogonal decomposition (4.10) with (4.11) in order to obtain the evolution system for the remainder terms (U, W) and for the modulation parameters (θ, ω, a). By analyzing the modulation equation for $a(t)$, we relate the rate of change of $a(t)$ and the value of the momentum functional $P(\Psi)$ given by (2.14).

Lemma 4.3. *Assume that the unique solution $\Psi \in C([0, t_0], H_\Gamma^1) \cap C^1([0, t_0], H_\Gamma^{-1})$ represented by (4.10) and (4.11) satisfies*

$$(4.12) \qquad |\omega(t) - 1| + \|U(t, \cdot) + iW(t, \cdot)\|_{H^1(\Gamma)} \le \epsilon, \quad t \in [0, t_0],$$

with $\epsilon \in (0, \delta_0)$ and δ_0 defined in (4.1). The time evolution of the translation parameter $a(t)$ is given by

$$(4.13) \qquad \dot{a}(t) = -\alpha_1^2 \omega^{-\frac{1}{2}} P(\Psi) \left[1 + \mathcal{O}(\|U + iW\|_{H^1(\Gamma)}) \right] + \mathcal{O}\left(\|U + iW\|_{H^1(\Gamma)}^2 \right),$$

where $P(\Psi)$ is given by (2.14).

Proof. By substituting (4.10) into the NLS equation (2.4) and by using the rotational and translation symmetries, we obtain the time evolution system for the remainder terms:

$$
\begin{aligned}
(4.14) \qquad \frac{d}{dt} \begin{pmatrix} U \\ W \end{pmatrix} &= \begin{pmatrix} 0 & L_-(\omega, a) \\ -L_+(\omega, a) & 0 \end{pmatrix} \begin{pmatrix} U \\ W \end{pmatrix} + (\dot{\theta} - \omega) \begin{pmatrix} W \\ -(\Phi_\omega + U) \end{pmatrix} \\
&\quad - \dot{\omega} \begin{pmatrix} \partial_\omega \Phi_\omega \\ 0 \end{pmatrix} - \dot{a} \begin{pmatrix} \Phi_\omega' \\ 0 \end{pmatrix} + \begin{pmatrix} -R_U \\ R_W \end{pmatrix},
\end{aligned}
$$

where $\Phi_\omega \equiv \Phi_\omega(x; a)$, the prime denotes derivative in x, the dot denotes derivative in t, the linearized operators are given by (3.3), and the residual terms are given by

$$(4.15) \qquad \begin{cases} R_U = 2\alpha^2 \left(2\Phi_\omega U + U^2 + W^2 \right) W, \\ R_W = 2\alpha^2 \left[\Phi_\omega(3U^2 + W^2) + (U^2 + W^2)U \right]. \end{cases}$$

By using the orthogonality conditions (4.11), we obtain the modulation equations for parameters (θ, ω, a) from the system (4.14):

$$(4.16) \qquad A \begin{bmatrix} \dot{\theta} - \omega \\ \dot{\omega} \\ \dot{a} \end{bmatrix} = \begin{bmatrix} 0 \\ 0 \\ -2\langle \Phi_\omega'(\cdot; a), W \rangle_{L^2(\Gamma)} \end{bmatrix} + \begin{bmatrix} \langle \Phi_\omega(\cdot; a), R_U \rangle_{L^2(\Gamma)} \\ \langle \partial_\omega \Phi_\omega, R_W \rangle_{L^2(\Gamma)} \\ -\langle (\cdot + a)\Phi_\omega(\cdot; a), R_W \rangle_{L^2(\Gamma)} \end{bmatrix},$$

where the matrix A is given by

$$A = \begin{bmatrix} \langle \Phi_\omega(\cdot; a), W \rangle_{L^2(\Gamma)} & -\langle \partial_\omega \Phi_\omega(\cdot; a), \Phi_\omega(\cdot; a) - U \rangle_{L^2(\Gamma)} & \langle \Phi_\omega'(\cdot; a), U \rangle_{L^2(\Gamma)} \\ \langle \partial_\omega \Phi_\omega(\cdot; a), \Phi_\omega(\cdot; a) + U \rangle_{L^2(\Gamma)} & -\langle \partial_\omega^2 \Phi_\omega(\cdot; a), W \rangle_{L^2(\Gamma)} & -\langle \partial_\omega \Phi_\omega'(\cdot; a), W \rangle_{L^2(\Gamma)} \\ -\langle (\cdot + a)\Phi_\omega(\cdot; a), W \rangle_{L^2(\Gamma)} & -\langle (\cdot + a)\partial_\omega \Phi_\omega(\cdot; a), U \rangle_{L^2(\Gamma)} & \langle (\cdot + a)\Phi_\omega(\cdot; a)', \Phi_\omega(\cdot; a) - U \rangle_{L^2(\Gamma)} \end{bmatrix}.$$

If $(U, W) = (0, 0)$, the matrix A is invertible since

$$A_0 = \begin{bmatrix} 0 & D_1(\omega) & 0 \\ -D_1(\omega) & 0 & 0 \\ 0 & 0 & -D_2(\omega) \end{bmatrix}$$

has nonzero elements thanks to (3.1) and (3.2). Therefore, under the assumption (4.12) with small $\epsilon > 0$, we have

$$\|A^{-1}\|_{\mathbb{M}_{3\times 3}} \leq C \tag{4.17}$$

for an ϵ-independent constant $C > 0$. This bound implies that the time evolution of the translation parameter $a(t)$ is given by

$$\dot{a} = \frac{2\langle \Phi'_\omega(\cdot; a), W\rangle_{L^2(\Gamma)}}{D_1(\omega)} \left[1 + \mathcal{O}(\|U + iW\|_{H^1(\Gamma)})\right] + \mathcal{O}\left(\|U + iW\|^2_{H^1(\Gamma)}\right). \tag{4.18}$$

On the other hand, the momentum functional $P(\Psi)$ in (2.14) can be computed at the solution Ψ in the orthogonal decomposition (4.10) as follows:

$$\begin{aligned}
P(\Psi) &= \langle \Phi_\omega(\cdot; a), W'\rangle_{L^2(\Gamma)} - \langle \Phi'_\omega(\cdot; a), W\rangle_{L^2(\Gamma)} + \mathcal{O}\left(\|U + iW\|^2_{H^1(\Gamma)}\right) \\
&= -2\langle \Phi'_\omega(\cdot; a), W\rangle_{L^2(\Gamma)} + \mathcal{O}\left(\|U + iW\|^2_{H^1(\Gamma)}\right),
\end{aligned} \tag{4.19}$$

where the integration by parts does not result in any contribution from the vertex at $x = 0$ thanks to the boundary conditions in (2.2) and the constraint (2.3). Combining (4.18) and (4.19) with the exact computation (3.2) yields expansion (4.13). ∎

Corollary 4.4. *In addition to (4.12), assume that Ψ_0 in (4.7) is chosen such that $P(\Psi_0) \geq C_0\delta$ with $C_0 > 0$. There exists ϵ_0 sufficiently small such that for every $\epsilon \in (0, \epsilon_0)$ there exists $\delta > 0$ such that the map $t \mapsto a(t)$ is strictly decreasing for $t \in [0, t_0]$.*

Proof. The map $t \mapsto P(\Psi)$ is monotonically increasing, as can be seen from the expression (2.15). Therefore, if the initial datum Ψ_0 in (4.7) satisfies $P(\Psi_0) \geq C_0\delta$, then

$$P(\Psi) \geq P(\Psi_0) \geq C_0\delta \quad \text{for all } t \in [0, t_0]. \tag{4.20}$$

It follows from (4.12), (4.13), and (4.20) that there exist δ- and ϵ-independent constants $C_1, C_2 > 0$ such that

$$-\dot{a} \geq C_1\delta - C_2\epsilon^2.$$

If δ satisfies $\delta \geq C\epsilon^2$ for a given small $\epsilon > 0$ with an ϵ-independent constant $C > C_1^{-1}C_2$, then $-\dot{a} \geq (C_1 C - C_2)\epsilon^2 > 0$ so that the map $t \mapsto a(t)$ is strictly decreasing for $t \in [0, t_0]$. ∎

4.3. Step 3: Energy estimates. The coercivity bound (3.8) in Lemma 3.1 allows us to control the time evolution of $\omega(t)$, $U(t, \cdot)$, and $W(t, \cdot)$, as long as $a(t)$ is bounded away from zero. The following result provides this control from energy estimates.

Lemma 4.5. *Let Ψ be the unique solution to the NLS equation (2.4) given by (4.10)–(4.11) for $t \in [0, t_0]$ with some $t_0 > 0$ such that the initial data $\Psi(0, \cdot) = \Psi_0$ satisfies (4.7)–(4.8). Assume that $a(t) \geq \bar{a}$ for $t \in [0, t_0]$. For every $\bar{a} > 0$, there exists a δ-independent positive constant $K(\bar{a})$ such that*

$$|\omega(t) - 1|^2 + \|U(t, \cdot) + iW(t, \cdot)\|^2_{H^1(\Gamma)} \leq K(\bar{a})\delta^2, \quad t \in [0, t_0]. \tag{4.21}$$

Proof. Recall that the shifted state $\Phi_\omega(\cdot; a)$ is a critical point of the action functional $\Lambda_\omega(\Psi) = E(\Psi) + \omega Q(\Psi)$ in (2.7). By using the decomposition (4.10) and the rotational invariance of the NLS equation (2.4), we define the following energy function:

$$\Delta(t) := E(\Phi_{\omega(t)} + U(t, \cdot) + iW(t, \cdot)) - E(\Phi)$$

(4.22)
$$+ \omega(t) \left[Q(\Phi_{\omega(t)} + U(t, \cdot) + iW(t, \cdot)) - Q(\Phi) \right].$$

Expanding Δ into Taylor series, we obtain

(4.23) $$\Delta = D(\omega) + \langle L_+(\omega, a)U, U \rangle_{L^2(\Gamma)} + \langle L_-(\omega, a)W, W \rangle_{L^2(\Gamma)} + N_\omega(U, W),$$

where $N_\omega(U, W) = O(\|U + iW\|^3_{H^1(\Gamma)})$ and $D(\omega)$ is defined by

$$D(\omega) := E(\Phi_\omega) - E(\Phi) + \omega \left[Q(\Phi_\omega) - Q(\Phi) \right].$$

Since $D'(\omega) = Q(\Phi_\omega) - Q(\Phi)$ thanks to the variational problem for the standing wave Φ_ω, we have $D(1) = D'(1) = 0$, and

(4.24) $$D(\omega) = (\omega - 1)^2 \langle \Phi, \partial_\omega \Phi_\omega|_{\omega=1} \rangle_{L^2(\Omega)} + \mathcal{O}(|\omega - 1|^3).$$

It follows from the initial decomposition (4.7)–(4.8) that

(4.25) $$\Delta(0) = E(\Phi + U_0 + iW_0) - E(\Phi) + Q(\Phi + U_0 + iW_0) - Q(\Phi)$$

satisfies the bound

(4.26) $$|\Delta(0)| \le C_0 \delta^2$$

for a δ-independent constant $C_0 > 0$. On the other hand, the energy and mass conservation in (2.5) imply that

(4.27) $$\Delta(t) = \Delta(0) + (\omega(t) - 1) \left[Q(\Phi + U_0 + iW_0) - Q(\Phi) \right],$$

where the remainder term also satisfies

(4.28) $$|Q(\Phi + U_0 + iW_0) - Q(\Phi)| \le C_0 \delta^2$$

for a δ-independent constant $C_0 > 0$. The representation (4.27) together with the expression (4.23) allows us to control $\omega(t)$ near $\omega(0) = 1$ and the remainder terms (U, W) in H^1_Γ as follows:

$$\Delta(0) = (\omega - 1)^2 \langle \Phi, \partial_\omega \Phi_\omega|_{\omega=1} \rangle_{L^2(\Omega)} - (\omega - 1) \left[Q(\Phi + U_0 + iW_0) - Q(\Phi) \right]$$

(4.29)
$$+ \langle L_+(\omega, a)U, U \rangle_{L^2(\Gamma)} + \langle L_-(\omega, a)W, W \rangle_{L^2(\Gamma)} + \mathcal{O}\left(|\omega - 1|^3 + \|U + iW\|^3_{H^1(\Gamma)}\right).$$

By using the expansion (4.29), the coercivity bound (3.8), and the bounds (4.26) and (4.28), we obtain

$$C_0 \delta^2 \ge \Delta(0) \ge \frac{1}{2\alpha_1^2 |\omega|^{\frac{1}{2}}} (\omega - 1)^2 - C_0 \delta^2 |\omega - 1| + C(\omega, a) \|U + iW\|^2_{H^1(\Gamma)}$$

$$+ \mathcal{O}\left(|\omega - 1|^3 + \|U + iW\|^3_{H^1(\Gamma)}\right),$$

from which the bound (4.21) follows. ■

Remark 4.6. By Remark 3.2, for every $\omega > 0$, we have $C(\omega, a) \to 0$ as $a \to 0$. Therefore, we have $K(\bar{a}) \to \infty$ as $\bar{a} \to 0$.

4.4. Proof of Theorem 2.8. The initial datum satisfies the initial decomposition (4.7)–(4.8) with small δ and initial conditions $\theta(0) = 0$, $\omega(0) = 1$, and $a(0) = a_0$ with $a_0 > 0$. Thanks to the continuous dependence of the solution of the NLS equation (2.4) on the initial datum, the solution is represented by the orthogonal decomposition (4.10)–(4.11) on a short time interval $[0, t_0]$ for some $t_0 > 0$. Hence, it satisfies the a priori bound (4.9). The modulation parameters $\theta(t)$, $\omega(t)$, and $a(t)$ are defined for $t \in [0, t_0]$ and $a(t) \geq \bar{a}$ for some $\bar{a} > 0$ for $t \in [0, t_0]$. By the energy estimates in Lemma 4.5, the parameter $\omega(t)$ and the remainder terms $(U, W) \in H_\Gamma^1$ satisfy the bound (4.21) with a δ-independent positive constant $K(\bar{a})$. For given small $\epsilon > 0$ and $\mathfrak{a} > 0$ in Theorem 2.8, let us define

$$(4.30) \qquad K_{\mathfrak{a}} := \max_{\bar{a} \in [\mathfrak{a}, a_0]} K(\bar{a}), \quad \delta := K_{\mathfrak{a}}^{-\frac{1}{2}} \epsilon.$$

Then, the bound (4.21) implies the bound (4.12) of Lemma 4.3 for all $t \in [0, t_0]$. Assume that the initial datum also satisfies $P(\Psi_0) \geq C_0 \delta$. By Corollary 4.4, the map $t \mapsto a$ is strictly decreasing for $t \in [0, t_0]$ if δ satisfies $\delta \geq C\epsilon^2$ for a δ and ϵ-independent constant $C > 0$. The definition of δ in (4.30) is compatible with the latter bound if $\epsilon \in (0, \epsilon_0)$ with

$$\epsilon_0 := \frac{1}{C\sqrt{K_{\mathfrak{a}}}}.$$

If in addition $\epsilon_0 \leq \delta_0$, where δ_0 is defined in Lemma 4.1, then the solution $\Psi(t, \cdot) \in H_\Gamma^1$ for $t \in [0, t_0]$ satisfies the conditions of Lemma 4.1 so that the orthogonal decomposition (4.10) with (4.11) is continued beyond the short time interval $[0, t_0]$ to the maximal time interval $[0, T]$ as long as $a(t) \geq \mathfrak{a}$ for $t \in [0, T]$. Thanks to the monotonicity argument in Lemma 4.3 and Corollary 4.4, for every $\epsilon \in (0, \epsilon_0)$, there exists a finite $T > 0$ such that $\lim_{t \to T} a(t) = \mathfrak{a}$. Note that $T = \mathcal{O}(\epsilon^{-2})$ as $\epsilon \to 0$. Theorem 2.8 is proved.

Remark 4.7. It follows that $K_{\mathfrak{a}} \to \infty$ as $\mathfrak{a} \to 0$ by Remark 4.6 so that $\epsilon_0 \to 0$ as $\mathfrak{a} \to 0$. As a result, it does not follow from Theorem 2.8 that the half-soliton $\Phi(\cdot; a = 0)$ is attained from the drifted shifted state $\Phi(\cdot; a(t))$ in a finite time.

Remark 4.8. If the initial datum $\Psi_0 \in H_\Gamma^1$ in (4.7) preserves the symmetry constraints (2.11), then the map $t \mapsto P(\Psi)$ is constant so that $P(\Psi) = P(\Psi_0)$. The condition $P(\Psi_0) \geq C_0 \delta$ with $C_0 > 0$ in Theorem 2.8 ensures that the shifted state $\Phi(\cdot; a(t))$ drifts toward the vertex at $x = 0$ even under the symmetry-preserving perturbations.

5. Instability of the half-soliton state. The proof of Theorem 2.9 is divided into several steps. First, we decompose the unique global solution Ψ to the NLS equation (2.4) into the modulated stationary state $\{e^{i\theta}\Phi_\omega\}_{\theta \in \mathbb{R}, \omega \in \mathbb{R}^+}$ and the symplectically orthogonal remainder terms, where $\Phi_\omega \equiv \Phi_\omega(\cdot; a = 0)$. Next, we provide a secondary decomposition of the remainder terms as a superposition of projections to the bases in X_ω and X_ω^* in (3.17) and (3.20) and the symplectically orthogonally remainder terms. We use energy estimates to control the time evolution of $\omega(t)$ and the remainder terms. Finally, we consider the perturbed Hamiltonian system for projections to the bases in X_ω and X_ω^* and prove that the truncated system is unstable near the zero equilibrium point. This instability drives the instability of the solution Ψ under the time flow of the NLS equation (2.4) away from the half-soliton state $\{e^{i\theta}\Phi_\omega\}_{\theta \in \mathbb{R}, \omega \in \mathbb{R}^+}$.

5.1. Step 1: Primary decomposition. For every sufficiently small $\delta > 0$, we consider the initial datum $\Psi_0 \in H_\Gamma^1$ to the Cauchy problem associated with the NLS equation (2.4) in the form

(5.1) $$\Psi_0 = \Phi + U_0 + iW_0, \quad \|U_0 + iW_0\|_{H^1(\Gamma)} \leq \delta,$$

subject to the orthogonality conditions

(5.2) $$\begin{cases} \langle W_0, \partial_\omega \Phi_\omega|_{\omega=1} \rangle_{L^2(\Gamma)} = 0, \\ \langle U_0, \Phi \rangle_{L^2(\Gamma)} = 0, \end{cases}$$

where $\Phi \equiv \Phi(\cdot; a = 0)$. By the global well-posedness theory [3, 20], this initial datum generates a unique global solution $\Psi \in C(\mathbb{R}, H_\Gamma^1) \cap C^1(\mathbb{R}, H_\Gamma^{-1})$ to the NLS equation (2.4).

We use the decomposition of the unique global solution $\Psi \in C(\mathbb{R}, H_\Gamma^1) \cap C^1(\mathbb{R}, H_\Gamma^{-1})$ into the modulated stationary state $\{e^{i\theta}\Phi_\omega\}_{\theta\in\mathbb{R},\omega\in\mathbb{R}^+}$ with ω close to $\omega_0 = 1$ and the symplectically orthogonal remainder terms. This decomposition is similar to Lemma 4.1 with $a_0 = 0$ with the only change that $a = 0$ is set in the decomposition (4.2) and the remainder terms satisfy the first two of the three orthogonality conditions in (4.3).

By continuity of the global solution and by Lemma 4.1, for every $\epsilon \in (0, \delta_0)$ with δ_0 defined in Lemma 4.1 there exists $t_0 > 0$ such that the unique solution Ψ satisfies

(5.3) $$\inf_{\theta\in\mathbb{R}} \|e^{-i\theta}\Psi(t, \cdot) - \Phi\|_{H^1(\Gamma)} \leq \epsilon, \quad t \in [0, t_0],$$

and can be uniquely represented as

(5.4) $$\Psi(t, x) = e^{i\theta(t)} \left[\Phi_{\omega(t)}(x) + U(t, x) + iW(t, x) \right],$$

subject to the orthogonality conditions

(5.5) $$\begin{cases} \langle W(t, \cdot), \partial_\omega \Phi_\omega|_{\omega=\omega(t)} \rangle_{L^2(\Gamma)} = 0, \\ \langle U(t, \cdot), \Phi_{\omega(t)} \rangle_{L^2(\Gamma)} = 0. \end{cases}$$

Since $\Psi \in C(\mathbb{R}, H_\Gamma^1) \cap C^1(\mathbb{R}, H_\Gamma^{-1})$ and the map $\mathbb{R} \ni \omega \mapsto \Phi_\omega \in H_\Gamma^1$ is smooth, we obtain $(\theta, \omega) \in C^1([0, t_0], \mathbb{R} \times \mathbb{R}^+)$, hence $U, W \in C([0, t_0], H_\Gamma^1) \cap C^1([0, t_0], H_\Gamma^{-1})$.

The choice (5.1) with (5.2) implies that $\omega(0) = 1$ and $\theta(0) = 0$. Although this is again special (see Remark 4.2), it is nevertheless sufficient for the proof of the instability result. In order to prove Theorem 2.9 we fix $\epsilon \in (0, \delta_0)$ and we intend to show that there exists $T > 0$ such that the bound (5.3) is satisfied for all $t \in [0, T)$ but fails for $t = T$ yielding the bound (2.18).

We substitute the decomposition (5.4) into the NLS equation (2.4) to get the time evolution system for the remainder terms (U, W). The following lemma reports the estimates on the evolution of the modulation parameters $\theta(t)$ and $\omega(t)$.

Lemma 5.1. *Assume that the unique solution* $\Psi \in C([0, t_0], H_\Gamma^1) \cap C^1([0, t_0], H_\Gamma^{-1})$ *represented by* (5.4) *and* (5.5) *satisfies*

(5.6) $$|\omega(t) - 1| + \|U(t, \cdot) + iW(t, \cdot)\|_{H^1(\Gamma)} \leq \epsilon, \quad t \in [0, t_0],$$

with $\epsilon \in (0, \delta_0)$ *and* δ_0 *defined in Lemma* 4.1. *There exists an* ϵ-*independent constant* $A > 0$ *such that for every* $t \in [0, t_0]$,

(5.7)
$$\begin{cases} |\dot{\theta}(t) - \omega(t)| \leq A \left(\|U(t, \cdot)\|_{H^1(\Gamma)}^2 + \|W(t, \cdot)\|_{H^1(\Gamma)}^2 \right), \\ |\dot{\omega}(t)| \leq A \|U(t, \cdot)\|_{H^1(\Gamma)} \|W(t, \cdot)\|_{H^1(\Gamma)}. \end{cases}$$

Proof. The time evolution system for the remainder terms is the same as the system (4.14) but with $a(t) = 0$ and $\dot{a}(t) = 0$ for $t \in [0, t_0]$. Using the orthogonality conditions (5.5) yields the same system of modulation equations as in (4.16) but constrained by the first two equations and a 2×2 coefficient matrix denoted by $\mathbf{A}$. The estimates (5.7) are obtained from invertibility of $\mathbf{A}$ satisfying $\|\mathbf{A}^{-1}\|_{\mathbb{M}_{2 \times 2}} \leq C$ for an ϵ-independent constant $C > 0$ and the explicit form of R_U and R_W in (4.15). ∎

5.2. Step 2: Secondary decomposition. Recall the eigenspaces X_ω and X_ω^* in (3.17) and (3.20). We decompose the remainder terms (U, W) in (5.4) as follows:

(5.8) $$U(t, x) = \sum_{j=1}^{N-1} c_j(t) U_{\omega(t)}^{(j)}(x) + U^\perp(t, x), \quad W(t, x) = \sum_{j=1}^{N-1} b_j(t) W_{\omega(t)}^{(j)}(x) + W^\perp(t, x),$$

subject to the orthogonality conditions for $U^\perp(t, \cdot) \in X_{\omega(t)}^*$ and $W^\perp(t, \cdot) \in X_{\omega(t)}$. The coefficients $c = (c_1, c_2, \ldots, c_{N-1}) \in \mathbb{R}^{N-1}$, $b = (b_1, b_2, \ldots, b_{N-1}) \in \mathbb{R}^{N-1}$ and the remainder terms $(U^\perp, W^\perp)$ in (5.8) are uniquely determined for each (U, W) due to the mutual orthogonality of the basis vectors used in Lemma 3.6. We also have $c, b \in C^1([0, t_0], \mathbb{R}^{N-1})$ and $U^\perp, W^\perp \in C([0, t_0], H_\Gamma^1) \cap C^1([0, t_0], H_\Gamma^{-1})$ since $\omega \in C^1([0, t_0], \mathbb{R})$ and $U, W \in C([0, t_0], H_\Gamma^1) \cap C^1([0, t_0], H_\Gamma^{-1})$.

Remark 5.2. Thanks to the explicit form (3.11), the parameter $c_1(t)$ in the decomposition (5.4) and (5.8) plays the same role as the parameter $a(t)$ in the decomposition (4.10), whereas $a(0) = a_0$ in the initial decomposition (4.7) is set to $a_0 = 0$.

By substituting (5.8) into the evolution equation for the remainder terms and using orthogonality conditions for the new remainder terms $U^\perp(t, \cdot) \in X_{\omega(t)}^*$ and $W^\perp(t, \cdot) \in X_{\omega(t)}$, we obtain the time evolution system for the coefficients in the form

(5.9)
$$\begin{cases} \left\langle W_\omega^{(j)}, U_\omega^{(j)} \right\rangle_{L^2(\Gamma)} \left(\frac{dc_j}{dt} - b_j \right) = R_c^{(j)}, \\ \left\langle W_\omega^{(j)}, U_\omega^{(j)} \right\rangle_{L^2(\Gamma)} \frac{db_j}{dt} = R_b^{(j)}, \end{cases}$$

with

$$R_c^{(j)} = \dot{\omega} \left[\left\langle \partial_\omega W_\omega^{(j)}, U^\perp \right\rangle_{L^2(\Gamma)} - \sum_{i=1}^{N-1} c_i \left\langle W_\omega^{(j)}, \partial_\omega U_\omega^{(i)} \right\rangle_{L^2(\Gamma)} \right]$$
$$+ (\dot{\theta} - \omega) \left\langle W_\omega^{(j)}, W \right\rangle_{L^2(\Gamma)} - \left\langle W_\omega^{(j)}, R_U \right\rangle_{L^2(\Gamma)},$$

$$R_b^{(j)} = \dot{\omega} \left[\left\langle \partial_\omega U_\omega^{(j)}, W^\perp \right\rangle_{L^2(\Gamma)} - \sum_{i=1}^{N-1} b_i \left\langle U_\omega^{(j)}, \partial_\omega W_\omega^{(i)} \right\rangle_{L^2(\Gamma)} \right]$$
$$- (\dot{\theta} - \omega) \left\langle U_\omega^{(j)}, U \right\rangle_{L^2(\Gamma)} + \left\langle U_\omega^{(j)}, R_W \right\rangle_{L^2(\Gamma)},$$

where the terms R_U and R_W are given by (4.15) and the orthogonality conditions

$$\left\langle U_\omega^{(j)}, \Phi_\omega \right\rangle_{L^2(\Gamma)} = \left\langle W_\omega^{(j)}, \partial_\omega \Phi_\omega \right\rangle_{L^2(\Gamma)} = 0, \quad 1 \le j \le N-1,$$

have been used. The time evolution system (5.9) will be truncated and studied in Step 3, whereas $\omega(t)$ and the remainder terms $(U^\perp, W^\perp)$ are controlled as small perturbations by using the energy estimates. The following lemma gives the estimates on these terms.

Lemma 5.3. *Assume that there exists a positive constant A such that for every $\epsilon > 0$ and some $t_0 > 0$, the remainder terms of the solution Ψ decomposed as (5.4) and (5.8) satisfy*

$$(5.10) \qquad |\omega(t) - 1| + \|c(t)\| + \|b(t)\| + \|U^\perp(t,\cdot) + iW^\perp(t,\cdot)\|_{H^1(\Gamma)} \le A\epsilon, \quad t \in [0, t_0].$$

There exist an ϵ-independent constant $C > 0$ such that

$$(5.11) \qquad |\omega(t) - 1|^2 + \|U^\perp(t,\cdot) + iW^\perp(t,\cdot)\|_{H^1(\Gamma)}^2 \le C \left(\delta^2 + \|b\|^2 + \|c\|^3 \right), \quad t \in [0, t_0],$$

where δ is given in (5.1) for the initial datum Ψ_0.

Proof. The expansion of the energy function (4.22) with the help of the explicit expressions in (2.5) implies that the term $N_\omega(U, W)$ in (4.23) can be written as

$$(5.12) \qquad N_\omega(U, W) = -4\langle \alpha^2 \Phi U, (U^2 + W^2) \rangle_{L^2(\Gamma)} + \mathcal{O}\left(\|U + iW\|_{H^1(\Gamma)}^4 \right).$$

Substituting the secondary decomposition (5.8) into the energy function (4.23) with the use of (5.12) yields

$$(5.13) \qquad \begin{aligned} \Delta &= D(\omega) + \langle L_+(\omega)U^\perp, U^\perp \rangle_{L^2(\Gamma)} + \langle L_-(\omega)W^\perp, W^\perp \rangle_{L^2(\Gamma)} + 2H_0(c, b) \\ &\quad + \widetilde{N}(\omega, c, b, U^\perp, W^\perp), \end{aligned}$$

where $H_0(c, b)$ is defined by

$$(5.14)$$

$$H_0(c, b) = \frac{1}{2} \sum_{j=1}^{N-1} \left\langle W^{(j)}, U^{(j)} \right\rangle_{L^2(\Gamma)} b_j^2 - 2 \sum_{j=1}^{N-1} \sum_{k=1}^{N-1} \sum_{n=1}^{N-1} \left\langle \alpha^2 \Phi U^{(j)}, U^{(k)} U^{(n)} \right\rangle_{L^2(\Gamma)} c_j c_k c_n,$$

and $\widetilde{N}(\omega, c, b, U^\perp, W^\perp)$ is bounded by

$$\begin{aligned} |\widetilde{N}(\omega, c, b, U^\perp, W^\perp)| \le A_1 \Big(&\|c\|^2 \|U^\perp\|_{H^1(\Gamma)} + \|U^\perp\|_{H^1(\Gamma)}^3 + \|c\|^4 + \|c\| \|b\|^2 + \|c\| \|W^\perp\|_{H^1(\Gamma)}^2 \\ &+ \|b\|^2 \|U^\perp\|_{H^1(\Gamma)} + \|U^\perp\|_{H^1(\Gamma)} \|W^\perp\|_{H^1(\Gamma)}^2 + |\omega - 1| \|b\|^2 + |\omega - 1| \|c\|^3 \Big) \end{aligned}$$

with ϵ-independent positive constant A_1. The expansion (5.13) also holds due to the Banach algebra property of $H^1(\Gamma)$ and the assumption (5.10). Combining the representations of Δ given by (4.27) and (5.13), we get

$$\begin{aligned} \Delta(0) - 2H_0(c, b) &= D(\omega) - (\omega - 1) \left[Q(\Phi + U_0 + iW_0) - Q(\Phi) \right] \\ &\quad + \langle L_+(\omega)U^\perp, U^\perp \rangle_{L^2(\Gamma)} + \langle L_-(\omega)W^\perp, W^\perp \rangle_{L^2(\Gamma)} + \widetilde{N}(\omega, c, b, U^\perp, W^\perp). \end{aligned}$$

Bounds (4.26) and (4.28) imply that there exists a δ-independent constant A_2 such that

$$|\Delta(0)| + |Q(\Phi + U_0 + iW_0) - Q(\Phi)| \le A_2\delta^2.$$

Moreover, it can be seen directly from (5.14) that $|H_0(c,b)| \le A_3(\|c\|^3 + \|b\|^2)$ for some generic positive constant A_3. By using the same estimates as in the proof of Lemma 4.5, a priori assumption (5.10) together with the coercivity bound (3.21) in Lemma 3.6 implies that there exists an ϵ-independent constant C in the bound (5.11). ∎

5.3. Step 3: The reduced Hamiltonian system. Estimates (5.7) in Lemma 5.1 and (5.11) in Lemma 5.3, as well as the representation of (R_U, R_W) in (4.15), imply that the time evolution system (5.9) is a perturbation of the following Hamiltonian system of degree $N-1$:

$$(5.15) \qquad \begin{cases} \langle W^{(j)}, U^{(j)} \rangle_{L^2(\Gamma)} \frac{d\gamma_j}{dt} = \frac{\partial H_0}{\partial \beta_j}, \\ \langle W^{(j)}, U^{(j)} \rangle_{L^2(\Gamma)} \frac{d\beta_j}{dt} = -\frac{\partial H_0}{\partial \gamma_j}, \end{cases}$$

where $H_0(\gamma, \beta)$ is the Hamiltonian given by (5.14). Direct computation with the help of the representations (3.11) and (3.12) in Lemma 3.5 implies that if $j \ge k > n$, then

$$\left\langle \alpha^2 \Phi U^{(j)}, U^{(k)} U^{(n)} \right\rangle_{L^2(\Gamma)} = \left(\frac{r_k}{\alpha_k} + \sum_{i=k+1}^{N} \frac{1}{\alpha_i^2} \right) \int_0^\infty \phi(\phi')^3 dx = 0$$

due to the explicit formula for r_k in (3.12). Therefore, one can rewrite the representation (5.14) for $H_0(\gamma, \beta)$ in the explicit form

$$(5.16) \qquad H_0(\gamma, \beta) = \frac{1}{2} \sum_{j=1}^{N-1} M_j b_j^2 - 2 \sum_{j=2}^{N-1} R_j \gamma_j^3 - 6 \sum_{j=1}^{N-1} \sum_{k>j}^{N-1} P_k \gamma_j \gamma_k^2,$$

where

$$M_j := \left\langle W^{(j)}, U^{(j)} \right\rangle_{L^2(\Gamma)},$$
$$R_j := \left\langle \alpha^2 \Phi U^{(j)}, U^{(j)} U^{(j)} \right\rangle_{L^2(\Gamma)},$$
$$P_k := \left\langle \alpha^2 \Phi U^{(j)}, U^{(k)} U^{(k)} \right\rangle_{L^2(\Gamma)}.$$

Note that the coefficient P_k is independent of j if $k > j$. Thanks to the construction of the eigenvectors in (3.11) and (3.12), the explicit expressions for coefficients R_j and P_k are given by

$$(5.17) \qquad R_j = \alpha_j^4 \left(\sum_{i=j}^{N} \frac{1}{\alpha_i^2} \right) \left(\sum_{i=j+1}^{N} \frac{1}{\alpha_i^2} \right) \left(\frac{1}{\alpha_j^2} - \sum_{i=j+1}^{N} \frac{1}{\alpha_i^2} \right) \int_0^\infty \phi(\phi')^3 dx$$

and

$$(5.18) \qquad P_k = \alpha_k^2 \left(\sum_{i=k}^{N} \frac{1}{\alpha_i^2} \right) \left(\sum_{i=k+1}^{N} \frac{1}{\alpha_i^2} \right) \int_0^\infty \phi(\phi')^3 dx.$$

It follows from (3.23) and (5.18) that $M_j > 0$ and $P_k < 0$ since $\phi(\phi')^3 < 0$ on $\mathbb{R}^+$. Also it follows from (2.3) and (5.17) that $R_1 = 0$.

The following lemma states that the zero equilibrium point is nonlinearly unstable in the reduced system (5.15) with the Hamiltonian (5.16).

Lemma 5.4. *There exists $\epsilon > 0$ such that for every sufficiently small $\delta > 0$, there is an initial point $(\gamma(0), \beta(0)) \in \mathbb{R}^{N-1} \times \mathbb{R}^{N-1}$ with $\|\gamma(0)\| + \|\beta(0)\| \le \delta$ such that the unique solution of the reduced Hamiltonian system (5.15) with (5.16) satisfies for some $t_0 > 0$: $\|\gamma(t_0)\| = \epsilon$ and $\|\gamma(t)\| > \epsilon$ for $t > t_0$. Moreover, if $\epsilon > 0$ is small, then $t_0 = \mathcal{O}(\epsilon^{-1/2})$, $\gamma(t) = \mathcal{O}(\epsilon)$, and $\beta(t) = \mathcal{O}(\epsilon^{3/2})$ for all $t \in [0, t_0]$.*

Proof. First, we claim that there exists an invariant subspace of solutions of the reduced Hamiltonian system (5.15) with (5.16) given by

$$(5.19) \qquad S := \{ \gamma_1 = C\gamma_2, \gamma_3 = \gamma_4 = \cdots = \gamma_{N-1} = 0 \}$$

for some constant $C \ne 0$. Indeed, eliminating β_j, we close the reduced system (5.15) on γ_j for every $j = 1, \ldots, N-1$:

$$(5.20) \qquad M_j \frac{d^2 \gamma_j}{dt^2} = 6R_j \gamma_j^2 + 12 \sum_{i=1}^{j-1} P_j \gamma_i \gamma_j + 6 \sum_{k=j+1}^{N-1} P_k \gamma_k^2.$$

It follows directly that $\gamma_3 = \gamma_4 = \cdots = \gamma_{N-1} = 0$ is an invariant solution of the last $(N-3)$ equations of system (5.20). Since $R_1 = 0$ from (2.3) and (5.17), the first two (remaining) equations of system (5.20) are given by

$$(5.21) \qquad \begin{cases} M_1 \frac{d^2 \gamma_1}{dt^2} = 6P_2 \gamma_2^2, \\ M_2 \frac{d^2 \gamma_2}{dt^2} = 6R_2 \gamma_2^2 + 12P_2 \gamma_1 \gamma_2. \end{cases}$$

The system is invariant on the subspace S in (5.19) if the constant C is a solution of the following quadratic equation:

$$2M_1 P_2 C^2 + M_1 R_2 C - M_2 P_2 = 0.$$

The quadratic equation admits two nonzero real solutions C if the discriminant is positive:

$$\mathcal{D} := M_1^2 R_2^2 + 8M_1 M_2 P_2^2 > 0,$$

which is true thanks to the positivity of M_1 and M_2 in (3.23). The reduced system (5.20) on the invariant subspace (5.19) yields the following scalar second-order equation:

$$(5.22) \qquad C^2 M_1 \frac{d^2 \gamma_1}{dt^2} - 6P_2 \gamma_1^2 = 0,$$

where $C \neq 0$, $M_1 > 0$, and $P_2 < 0$. The zero equilibrium $(\gamma_1, \dot{\gamma}_1) = (0, 0)$ is a cusp point so that it is unstable in the nonlinear equation (5.22).

Next, we prove the assertion of the lemma. For every sufficiently small $\delta > 0$, we choose the initial point $(\gamma(0), \beta(0)) \in \mathbb{R}^{N-1} \times \mathbb{R}^{N-1}$ in the invariant subspace S in (5.19) satisfying $\|\gamma(0)\| + \|\beta(0)\| \leq \delta$. Since $(0, 0)$ is a cusp point in the reduced equation (5.22) there exists a $t_0 > 0$ such that $\|\gamma(t_0)\| = \epsilon$ and $\|\gamma(t)\| > \epsilon$ for $t > t_0$ for any fixed $\epsilon > 0$.

Let us consider a fixed sufficiently small value of $\epsilon > 0$. We have $\gamma(t) = \mathcal{O}(\epsilon)$ for $t \in [0, t_0]$ by the construction. Setting $\dot{\gamma}_1 = \beta_1$, the evolution equation (5.22) implies that for every $t \in [0, t_0]$ there is an (ϵ, δ)-independent constant $A > 0$ such that

$$\begin{cases} |\gamma_1(t)| \leq \left| \int_0^t \beta_1(s) ds \right| + |\gamma_1(0)| \leq A\epsilon^{3/2} t_0 + \delta, \\ |\beta_1(t)| \leq A \left| \int_0^t \gamma_1^2(s) ds \right| + |\beta_1(0)| \leq A\epsilon^2 t_0 + \delta. \end{cases}$$

If $\delta \in (0, A\epsilon^{3/2})$, then $\gamma_1(t) = \mathcal{O}(\epsilon)$ and $\beta_1(t) = \mathcal{O}(\epsilon^{3/2})$ holds for $t \in [0, t_0]$ with $t_0 = \mathcal{O}(\epsilon^{-1/2})$. The assertion of the lemma is proven. ∎

By Lemma 5.4, there exists a trajectory of the finite-dimensional system (5.15) near the zero equilibrium which leaves the ϵ-neighborhood of the zero equilibrium over the time span $[0, t_0]$ with $t_0 = \mathcal{O}(\epsilon^{-1/2})$. Moreover, we have $\gamma(t) = \mathcal{O}(\epsilon)$ and $\beta(t) = \mathcal{O}(\epsilon^{3/2})$ for every $t \in [0, t_0]$. This scaling suggests we consider the following region in the phase space $\mathbb{R}^{N-1} \times \mathbb{R}^{N-1}$ of the evolution system (5.9) in variables (c, b):

$$(5.23) \qquad \|c(t)\| \leq A\epsilon, \quad \|b(t)\| \leq A\epsilon^{3/2}, \quad t \in [0, t_0],$$

where $t_0 \leq A\epsilon^{-1/2}$, for an ϵ-independent constant $A > 0$. Vectors (c, b) in the region (5.23) still satisfy the bound (5.10), hence the decompositions (5.4) and (5.8) remain valid due to the bound (5.11) in Lemma 5.3. The following result proved in [19] shows that a trajectory of system (5.9) closely follows the trajectory of the finite-dimensional system (5.15) in the region (5.23).

Lemma 5.5. *For $\epsilon > 0$ sufficiently small, assume that the remainder terms of the solution Ψ decomposed as (5.4) and (5.8) satisfy (5.10) and let $(\gamma, \beta) \in C^1([0, t_0], \mathbb{R}^{N-1} \times \mathbb{R}^{N-1})$ be a solution to the reduced system (5.15) in the region (5.23). The solution $(c, b) \in C^1([0, t_0], \mathbb{R}^{N-1} \times \mathbb{R}^{N-1})$ to the evolution system (5.9) with initial datum $c(0) = \gamma(0)$ and $b(0) = \beta(0)$ remains in the region (5.23) and there exists a generic ϵ-independent constant $A > 0$ such that*

$$(5.24) \qquad \|c(t) - \gamma(t)\| \leq A\epsilon^{3/2}, \quad \|b(t) - \beta(t)\| \leq A\epsilon^2, \quad t \in [0, t_0].$$

Remark 5.6. By the bound (5.24), $c_1(t)$ closely follows $\gamma_1(t)$, whereas by the first equation of system (5.21) with $M_1 > 0$ and $P_2 < 0$, the map $t \mapsto \gamma_1(t)$ is monotonically decreasing if $\gamma_1'(0) \leq 0$. Thanks to the correspondence between $c_1(t)$ and $a(t)$ in Remark 5.2, this corresponds to the irreversible drift of the parameter $a(t)$ toward smaller values in Corollary 4.4. Compared to Corollary 4.4, the irreversible drift is observed from the half-soliton state with $a(0) = a_0 = 0$.

5.4. Proof of Theorem 2.9. Let us consider the unstable solution of the reduced system (5.15) according to Lemma 5.4. This solution belongs to the region (5.23) and, by Lemma 5.5, the correction terms satisfy (5.24). Therefore, the solution of system (5.9) still satisfies the bound (5.23) over the time span $[0, t_0]$ with $t_0 = \mathcal{O}(\epsilon^{-1/2})$.

For every $\epsilon > 0$, we set $\delta \in (0, A\epsilon^{3/2})$ and use Lemma 5.3 to control the terms ω, $U^\perp$, and $W^\perp$ by the bound (5.11). Therefore, the solution given by decompositions (5.4) and (5.8) satisfies the bound (5.3) for $t \in [0, t_0]$.

Since the solution γ to the reduced system (5.15) grows in time and reaches the boundary in the region (5.23) by Lemma 5.4, the bound (5.24) implies that the same is true for the solution $c(t)$ of system (5.9). Hence, for every fixed $\epsilon > 0$ (sufficiently small), the initial data Ψ_0 satisfying the bound (5.1) with $\delta \in (0, A\epsilon^{3/2})$ generates the unique solution Ψ of the NLS equation (2.4) which reaches and crosses the boundary in (5.3) for some $t_0 = \mathcal{O}(\epsilon^{-1/2})$. Theorem 2.9 is proved.

6. Numerical verification. Here we describe numerical experiments that illustrate the implications of Theorems 2.8 and 2.9. Note that in all figures, we plot $U = (u_1, u_2, \ldots, u_N)$ with the components

$$u_j(x) = \alpha_j \psi_j(x).$$

Under the boundary conditions in (2.1), the solution U is continuous across the vertex. The shifted state of Lemma 2.2 with parameter $a \in \mathbb{R}$ is given in the variable U by $\alpha\Phi(\cdot; a)$.

6.1. Numerical method. We briefly describe the numerical method used to simulate time-dependent solutions of the NLS equation (2.4). Each semi-infinite edge is truncated to a finite length L, with Dirichlet boundary conditions imposed at the leaf endpoint. The spatial derivatives are discretized using second-order centered differences. The derivative boundary conditions in (2.2) are enforced using ghost points. That is, if the spacing between the grid points on edge j is given by Δx_j, then the grid points are located at $x_k^{(j)} = (k - \frac{1}{2})\Delta x_j$. There is no grid point at the vertex: instead along each edge there is a *ghost point* located at $x_0^{(1)} = \Delta x_1/2$ and $x_0^{(j)} = -\Delta x_j/2$ for $j = 2, \ldots, N$. The values at the ghost points are determined by enforcing the discretized boundary condition with the value at the vertex approximated by linear interpolation.

Time evolution is calculated using a second-order split-step method following Weidemann and Herbst [35]. The linear and nonlinear parts of the evolution are handled separately, with an explicit phase rotation with time step Δt sandwiched between two steps of the linear part with time steps of $\Delta t/2$ using the Crank–Nicolson scheme.

While the simulations are primarily concerned with the behavior of solutions concentrated away from the computational boundary, the evolution naturally gives rise to radiation, which quickly propagates to the boundary. This radiation interacts with the computational boundaries and leads to numerical instability that effects the computational results. Following Nissen and Kreiss [22], perfectly matched layers are used at the leaf endpoints to absorb this radiation. In practice, this leads to a modification of the discretized Laplacian at a finite number of points near the leaf vertices.

Standard care is taken to ensure the accuracy of the numerical simulations including quantitative convergence study and the tracking of conserved quantities.

6.2. Experiments with eigenfunction perturbation. We consider the balanced star graph with one incoming edge and two outgoing edges. For simplicity, we also assume $\alpha_2 = \alpha_3$. For the shifted state of Lemma 2.2, the spectrum of linearized operator $L_+(\omega, a)$ is shown in Figure 2. In particular, for $\omega = 1$, the operator possesses a negative eigenvalue $\lambda_0 = -3$ for all a, and a second eigenvalue $\lambda_1(a)$ for $a < a_*$, which is positive for $0 < a < a_*$ and negative for $a < 0$. Thus the Morse index suggests that the shifted state is linearly stable when $a > 0$ and linearly unstable when $a < 0$.

Let U_a be the eigenfunction of the operator $L_+(\omega, a)$ associated with the eigenvalue λ_1, which exists for every $a < a_*$, and let it be normalized by $\|U_a\|_{L^2(\Gamma)} = 1$. We consider the initial datum to the NLS equation (2.4) of the form

$$(6.1) \qquad\qquad \Psi_0 = \Phi(\cdot; a) + \epsilon U_a.$$

We assume here that $U_a(x) = 0$ on edge one, $U_a(x) < 0$ on edge two, and $U_a(x) > 0$ on edge three. Such an initial datum has the initial momentum $P(\Psi_0) = 0$ regardless of whether ϵ is real or has nonzero imaginary part.

We first present a simulation of the unstable shifted state with $a = -0.55$ and $\epsilon = 0.1$, in which the nonmonotonic part lies on the two outgoing edges. The time-dependent solution is plotted in Figure 3. The solution on edge three is initially slightly larger than on edge two. This asymmetry grows until the solution has concentrated on edge three, and then propagates away from the vertex along edge three. A lower-amplitude traveling wave, not visible in this plot, propagates away from the vertex on edge two.

The behavior is more interesting when we consider the stable shifted state with $a = 0.55 > 0$ and $\epsilon = 0.1$, in which the nonmonotonic part lies on the only incoming edge. The shifted state is linearly stable but Theorem 2.8 predicts drift of this shifted state toward smaller values of a, where Theorem 2.9 predicts nonlinear instability once the vertex is reached. The left panels of Figure 4 show that for $0 < t \lesssim 40$, the dynamics is very slow. After $t \approx 40$, the shifted state quickly propagates away from the vertex along edge two.
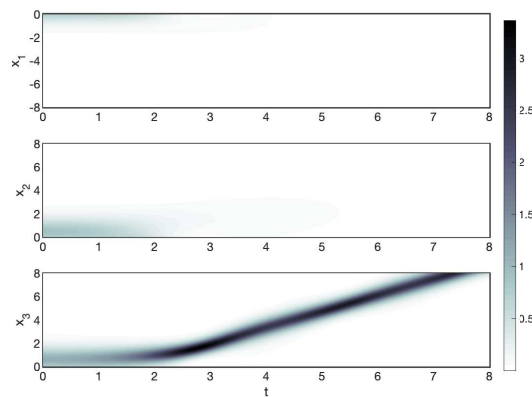
Figure 3. *A numerical solution with initial datum* (6.1) *for $a = -0.55$ and $\epsilon = 0.1$. The colorbar corresponds to values of $|u|^2$. The three panels correspond to the solution on edges one, two, and three going down.*
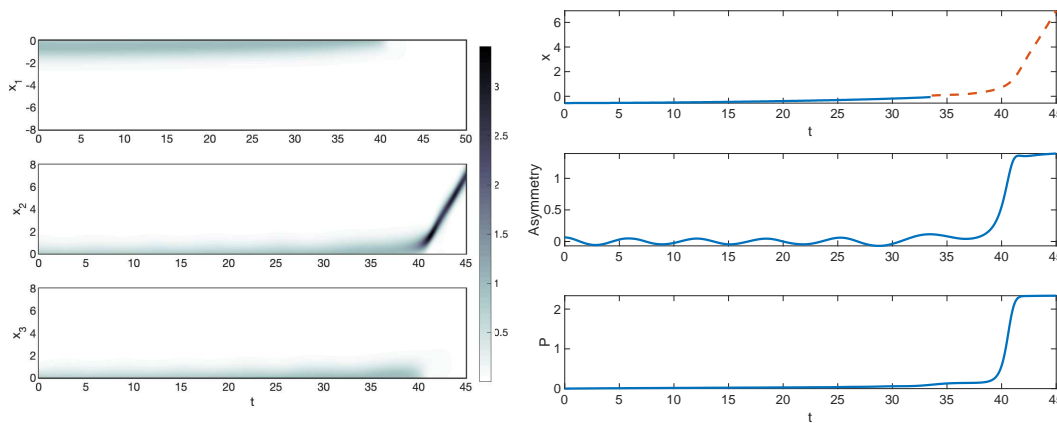
Figure 4. *Left: A numerical solution with initial datum* (6.1) *for $a = 0.55$ and $\epsilon = 0.1$. The colorbar corresponds to values of $|u|^2$. Right: Postprocessed quantities form the same simulation. (Top) The position of the maximum of u. The solid line for $t < 33.5$ describes the position on the incoming edge one. The dashed line for $t > 33.5$ shows the position of the maximum on edge two. (Middle) The asymmetry, defined as $\|u_2\|_{L^2(\mathbb{R}^+)} - \|u_3\|_{L^2(\mathbb{R}^+)}$. (Bottom) The momentum $P(\Psi)$ versus time t.*

The right panels of Figure 4 show some quantities postprocessed from the simulation. The top panel shows the location of the numerical maximum of $|u|$. At about $t = 33.5$, the maximum crosses from edge one to edge two at $x = 0$. The second panel shows the $\|u_2\|_{L^2(\mathbb{R}^+)} - \|u_3\|_{L^2(\mathbb{R}^+)}$, the difference between L^2 norms along the two outgoing edges, which is used as a proxy for the amplitude of the eigenfunction perturbation. This quantity oscillates between positive and negative values while the shifted state lies along the incoming edge, corresponding to stable evolution. It enters a period of exponential growth for $38 \lesssim t \lesssim 40$, once the shifted state has moved to the outgoing edges. During this period, a high-amplitude state forms on edge two and a low-amplitude state on edge three. The bottom panel shows that the momentum grows slowly until $t \approx 33.5$, then grows quickly, before saturating at $t \approx 42$, and moving with constant momentum thereafter.

This numerical simulation shows that perturbations to a shifted state with $a > 0$ grow subexponentially, consistent with the drift instability of Theorem 2.8. Similarly, postprocessing the simulation shown in Figure 3 with $a < 0$ shows that the perturbation immediately grows at an exponential rate, consistent with a linear instability proven in [20].

6.3. Experiments with other perturbations. Initial data of type (6.1) exist for $a < a_* \approx 0.66$ only if $\omega = 1$. However, we found almost identical dynamics as above by perturbing a shifted state with $a > a_*$, by a function similar to U_a which vanishes on the incoming edge, and takes the form $\pm cxe^{-\lambda x}$ on the two outgoing edges. We will not report further on such simulations.

All initial data of type (6.1) have zero initial momentum $P(\Psi_0) = 0$. An interesting question is what happens when we apply a perturbation such that the initial datum gives $P(\Psi_0) < 0$. Equation (2.15) implies that the map $t \mapsto P(\Psi)$ is increasing. Therefore, the question is whether the shifted states propagating along the incoming edge away from the vertex initially can escape the drift instability.
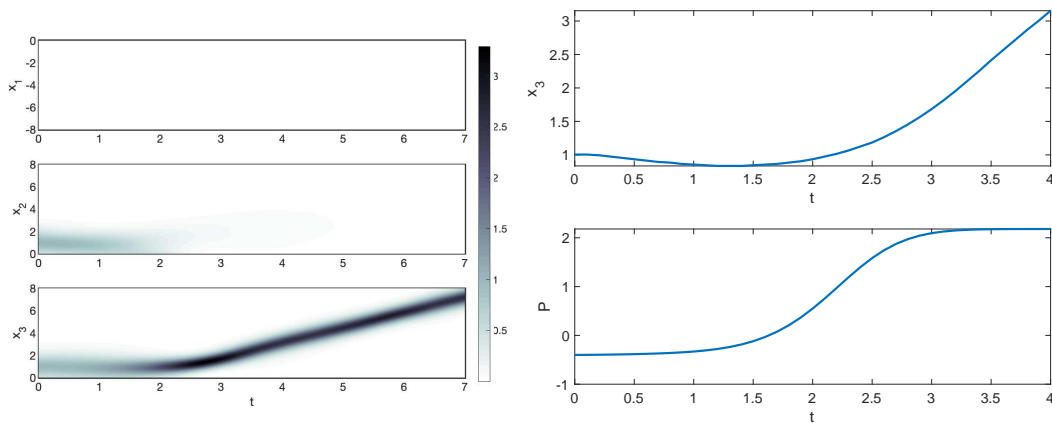
Figure 5. *A numerical solution with initial datum* (6.2) *for $a = -1$ and $\mu = 0.1i$. Details as in Figure* 4.
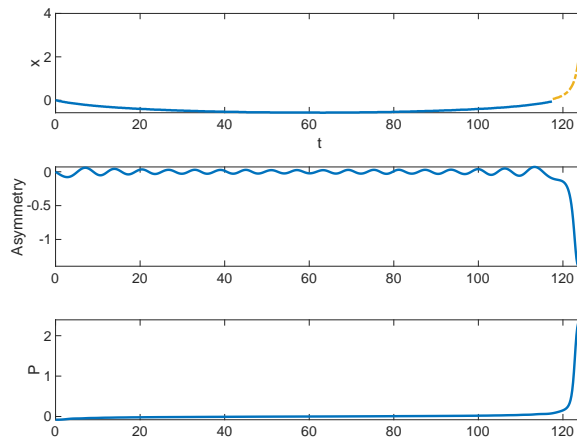

Figure 6. *A numerical solution with initial datum* (6.2) *for $a = 0$ and $\mu = -0.02i$. (Top) The position of the maximum of $|u|$, on edge one for $t < 117$ and on edge three (dashed) for $t > 117$. (Middle) Asymmetry of the solution between the two outgoing edges. (Bottom) The momentum $P(\Psi)$ versus time t.*

We construct perturbed shifted states as follows. Choose $\mu \in \mathbb{C}$ and define Ψ_0 by

$$(6.2) \qquad \begin{cases} \psi_1(x) = \alpha_1^{-1} e^{\mu x} \phi(x + a), \\ \psi_2(x) = \alpha_2^{-1} e^{2\mu x} \phi(x + a), \\ \psi_3(x) = \alpha_3^{-1} \phantom{e^{2\mu x}} \phi(x + a). \end{cases}$$

If μ is small, then $\Psi_0 \in H_\Gamma^2$ and $\|\Psi_0 - \Phi(\cdot; a)\|$ is small. The initial datum has nonzero initial momentum $P(\Psi_0) \neq 0$ if $\mathrm{Im}(\mu) \neq 0$.

We perform such a simulation with $a = -1$ and pure imaginary $\mu = 0.1i$. This slowly modulates the phase of the shifted state while keeping the amplitude at each point unchanged. The solution has its maxima on the outgoing edges and has negative initial momentum $P(\Psi_0) < 0$, so initially it propagates toward the vertex. Figure 5 shows that the numerical solution quickly concentrates on edge three and begins propagating away from the vertex. This is more visible in the right panel, which shows the location of the maximum value on edge three, which ini-

tially decreases, before increasing, and the momentum, which is initially negative, but which rapidly becomes positive.

A final simulation shows a solitary wave that travels away from the vertex along the incoming edge before reversing direction, crossing the vertex and escaping to infinity along one of the outgoing edges, shown in Figure 6. The simulation was performed with initial datum of form (6.2) with $a = 0$ and $\mu = -0.02\, i$. The initial datum differs from the half-soliton state Φ by 0.04 in L^2-norm, hence it can be considered as a small perturbation of the half-soliton state. The initial momentum is $P(\Psi_0) = -0.08$. The solution gradually slows down, with the momentum vanishing at about $t = 62$. The maximum crosses the vertex at about $t = 117$ and at this point the solution concentrates on edge three and the momentum begins increasing rapidly.

7. Conclusion. This paper concludes the study of the NLS equation on a balanced star graph originated in [19, 20]. We have proven analytically and illustrated numerically that symmetry-breaking perturbations induce instability of the shifted state in the time evolution. When the shifted state has a monotonic tail on the only incoming edge, it is spectrally unstable and the perturbations grow exponentially fast. When the shifted state has monotonic tails on the $(N-1)$ outgoing edges, it is spectrally stable but nonlinearly unstable. The perturbations do not grow in time but the center of mass of the shifted state drifts slowly along the incoming edge toward the vertex. This drift is induced by the irreversible growth of momentum in the time evolution due to the broken translational symmetry at the vertex point. Once the center of mass for the shifted state reaches the vertex, the perturbations start to grow faster, first algebraically and then exponentially. The numerical simulations not only verify the outcomes of the nonlinear dynamics predicted by the main theorems (Theorems 2.8 and 2.9) but also illustrate how generic this phenomenon is on the balanced star graphs.

REFERENCES

[1] R. ADAMI, C. CACCIAPUOTI, D. FINCO, AND D. NOJA, *On the structure of critical energy levels for the cubic focusing NLS on star graphs*, J. Phys. A., 45 (2012), 192001.

[2] R. ADAMI, C. CACCIAPUOTI, D. FINCO, AND D. NOJA, *Constrained energy minimization and orbital stability for the NLS equation on a star graph*, Ann. Inst. H. Poincaré Anal. Non Linéaire, 31 (2014), pp. 1289–1310.

[3] R. ADAMI, C. CACCIAPUOTI, D. FINCO, AND D. NOJA, *Variational properties and orbital stability of standing waves for NLS equation on a star graph*, J. Differential Equations, 257 (2014), pp. 3738–3777.

[4] R. ADAMI, C. CACCIAPUOTI, D. FINCO, AND D. NOJA, *Stable standing waves for a NLS on star graphs as local minimizers of the constrained energy*, J. Differential Equations, 260 (2016), pp. 7397–7415.

[5] R. ADAMI, E. SERRA, AND P. TILLI, *NLS ground states on graphs*, Calc. Var., 54 (2015), pp. 743–761.

[6] R. ADAMI, E. SERRA, AND P. TILLI, *Threshold phenomena and existence results for NLS ground states on graphs*, J. Funct. Anal., 271 (2016), pp. 201–223.

[7] R. ADAMI, E. SERRA, AND P. TILLI, *Multiple positive bound states for the subcritical NLS equation on metric graphs*, Calc. Var. Partial Differential Equations, 58 (2019), 5.

[8] J. ANGULO PAVA AND N. GOLOSHCHAPOVA, *On the orbital instability of excited states for the NLS equation with the δ-interaction on a star graph*, Discrete Contin. Dyn. Syst., 38 (2018), pp. 5039–5066.

[9] J. ANGULO PAVA AND N. GOLOSHCHAPOVA, *Extension theory approach in the stability of the standing waves for the NLS equation with point interactions on a star graph*, Adv. Differential Equations, 23 (2018), pp. 793–846.

[10] C. CACCIAPUOTI, S. DOVETTA, AND E. SERRA, *Variational and stability properties of constant solutions to the NLS equation on compact metric graphs*, Milan J. Math., 86 (2018), pp. 305–327.

[11] V. CAUDRELIER, *On the inverse scattering method for integrable PDEs on a star graph*, Commun. Math. Phys., 338 (2015), pp. 893–917.

[12] S. CUCCAGNA, *On instability of excited states of the nonlinear Schrödinger equation*, Phys. D, 238 (2009), pp. 38–54.

[13] S. CUCCAGNA AND M. MAEDA, *On orbital instability of spectrally stable vortices of the NLS in the plane*, J. Nonlinear Sci., 26 (2016), pp. 1851–1894.

[14] S. DOVETTA, *Existence of infinitely many stationary solutions of the L^2-subcritical and critical NLSE on compact metric graphs*, J. Differential Equations, 264 (2018), pp. 4806–4821.

[15] S. GILG, D. E. PELINOVSKY, AND G. SCHNEIDER, *Validity of the NLS approximation for periodic quantum graphs*, Nonlin. Diff. Eqs. Applic., 23 (2016), 63.

[16] R. H. GOODMAN, *NLS bifurcations on the bowtie combinatorial graph and the dumbbell metric graph*, Discrete Contin. Dyn. Syst. Ser. A, 39 (2019), pp. 2203–2232.

[17] M. GRILLAKIS, J. SHATAH, AND W. STRAUSS, *Stability theory of solitary waves in the presence of symmetry*, J. Funct. Anal., 74 (1987), pp. 160–197.

[18] A. KAIRZHAN, *Orbital instability of standing waves for NLS equation on star graphs*, Proc. Amer. Math. Soc., 147 (2019), pp. 2911–2924.

[19] A. KAIRZHAN AND D. PELINOVSKY, *Nonlinear instability of half-solitons on star graphs*, J. Differential Equations, 264 (2018), pp. 7357–7383.

[20] A. KAIRZHAN AND D. E. PELINOVSKY, *Spectral stability of shifted states on star graphs*, J. Phys. A, 51 (2018), 095203.

[21] J. MARZUOLA AND D. E. PELINOVSKY, *Ground states on the dumbbell graph*, Appl. Math. Res. Express. AMRX, 2016 (2016), pp. 98–145.

[22] A. NISSEN AND G. KREISS, *An optimized perfectly matched layer for the Schrödinger equation*, Commun. Comput. Phys., 9 (2015), pp. 147–179.

[23] D. NOJA, *Nonlinear Schrödinger equation on graphs: Recent results and open problems*, Philos. Trans. A, 372 (2014), 20130002.

[24] D. NOJA, D. PELINOVSKY, AND G. SHAIKHOVA, *Bifurcations and stability of standing waves on tadpole graphs*, Nonlinearity, 28 (2015), pp. 2343–2378.

[25] D. NOJA, S. ROLANDO, AND S. SECCHI, *Standing waves for the NLS on the double-bridge graph and a rational-irrational dichotomy*, J. Differential Equations, 266 (2019), pp. 147–178.

[26] A. PANKOV, *Nonlinear Schrödinger equations on periodic metric graphs*, Discrete Contin. Dyn. Syst., 38 (2018), pp. 697–714.

[27] D. E. PELINOVSKY AND G. SCHNEIDER, *Bifurcations of standing localized waves on periodic graphs*, Ann. Henri Poincaré, 18 (2017), pp. 1185–1211.

[28] K. K. SABIROV, D. B. BABAJANOV, D. U. MATRASULOV, AND P. G. KEVREKIDIS, *Dynamics of Dirac solitons in networks*, J. Phys. A, 51 (2018), 435203.

[29] E. SERRA AND L. TENTARELLI, *Bound states of the NLS equation on metric graphs with localized nonlinearities*, J. Differential Equations, 260 (2016), pp. 5627–5644.

[30] E. SERRA AND L. TENTARELLI, *On the lack of bound states for certain NLS equations on metric graphs*, Nonlinear Anal., 145 (2016), pp. 68–82.

[31] J. SHATAH AND W. STRAUSS, *Spectral condition for instability*, Contemp. Math,. 255 (2000), pp. 189–198.

[32] Z. SOBIROV, D. BABAJANOV, D. MATRASULOV, K. NAKAMURA, AND H. UECKER, *Sine–Gordon solitons in networks: Scattering and transmission at vertices*, Europhys. Lett., 115 (2016), 50002.

[33] Z. SOBIROV, D. MATRASULOV, K. SABIROV, S. SAWADA, AND K. NAKAMURA, *Integrable nonlinear Schrödinger equation on simple networks: Connection formula at vertices*, Phys. Rev. E, 81 (2010), 066602.

[34] L. TENTARELLI, *NLS ground states on metric graphs with localized nonlinearities*, J. Math. Anal. Appl., 433 (2016), pp. 291–304.

[35] J. A. C. WEIDEMAN AND B. M. HERBST, *Split-step methods for the solution of the nonlinear Schrödinger equation*, SIAM J. Numer. Anal., 23 (1986), pp. 485–507.

[36] M. I. WEINSTEIN, *Modulation stability of ground states of nonlinear Schrödinger equations*, SIAM J. Math. Anal., 16 (1985), pp. 472–491.

[37] M. I. WEINSTEIN, *Liapunov stability of ground states of nonlinear dispersive evolution equations*, Comm. Pure Appl. Math., 39 (1986), pp. 51–68.

[38] J. R. YUSUPOV, K. K. SABIROV, M. EHRHARDT, AND D. U. MATRASULOV, *Transparent quantum graphs*, Phys. Lett. A, 383 (2019), pp. 2382–2388.